Lithium-ion batteries and the transition to electric vehicles: environmental challenges and opportunities from a life cycle perspective

Xu, C.

5 Electric vehicle batteries alone could satisfy short-term grid storage demand by as early as 2030[d]

Abstract

The energy transition will require a rapid deployment of renewable energy (RE) and electric vehicles (EVs) where mass transit or personal transit options are unavailable. EV battery storage could complement variable RE generation by providing short-term grid services. However, estimating the market size of this opportunity requires an understanding of many socio-technical parameters and constraints. We quantify global EV battery capacity available for grid storage using an integrated model which incorporates future EV battery deployment, battery degradation, and market participation rates. We include both the 'in-use' and 'end-of-life' potential of EV batteries. We find a technical capacity of 32-62 TWh by 2050 and that modest market participation rates (12%-43%) are needed to provide most if not all short-term grid storage demand globally. This demand could be met as early as 2030 across most regions. Our estimates are generally conservative and offer a lower bound of future opportunities.

5.1 Introduction

Electrification and the rapid deployment of renewable energy (RE) generation are both critical to a low-carbon energy transition[56,73]. They also address many other environmental issues, including air pollution. However, the variability of critical RE technologies, wind and solar, combined with increasing electrification may present a challenge to grid stability and security of supply[56,73]. To address this, there are several supply-side options for meeting demand including, in approximate ascending order of today's estimated cost: energy storage, firm electricity generators (such as nuclear or geothermal generators), long-distance electricity transmission to balance variations, over-building of RE (resulting in curtailment in periods of lower demand), and power-to-gas[188]. In addition to these supply-side options, demand-side management is also

[d] Under the second revision with Nature Communications, as: Xu, C., Behrens, P., Gasper, P., Smith, K., Hu, M., Tukker, A. & Steubing, B. Electric vehicle batteries alone could satisfy short-term grid storage demand by as early as 2030.

vital in shifting and flattening peak demand[189]. Given rapid cost declines, batteries are one of the major options for energy storage and can be used in various grid-related applications to improve grid performance. These declines in cost have also driven a cost-decline of EVs. Given that many batteries will be produced for light-duty transport these could offer a cost- and materially-efficient approach for the short-term storage requirements needed on electricity grids across the world[190].

EV batteries can be used while they are part of the vehicle in vehicle-to-grid approaches, or after the end of the life (EoL) of the vehicle (when they are removed and used separately to the chassis). Vehicle-to-grid charging can be smart to enable dynamic EV charging and load-shifting services to the grid. EVs can also be used to store electricity and deliver it to the grid at peak times when power generation is more expensive[14]. These opportunities rely on standards and market arrangements that allow for dynamic energy pricing and the ability of owners to benefit from the value to the grid (value that can include deferred or avoided capital expenditure on additional stationary storage, power electronic infrastructure, transmission build-out *etc*[14]).

There will also be substantial grid-based value for EV batteries at vehicle EoL (hereafter called retired batteries). Usually, when the remaining battery capacity drops to between 70-80% of the original capacity batteries become unsuitable for use in EVs[15]. However, these retired batteries may still have years of useful life in less demanding stationary energy storage applications[16]. These batteries can continue to buffer differences in supply and demand and contribute to grid stability.

The utilization of EV batteries could improve the flexibility of supply while reducing the capital costs and material-related emissions associated with additional storage and power-electronic infrastructure. However, the total grid storage capacity of EV batteries depends on different socio-economic and technical factors such as business models, consumer behaviour (in driving and charging), battery degradation, and more[53,54]. Investigating the future grid storage capacity of EV batteries is essential in understanding the role EV batteries could play in the energy transition. Previous global-level studies, including those on vehicle-to-grid capacity[55-57] and retired battery capacity[57,58], while informative, rarely consider several important factors such as: non-linear, empirically-based battery degradation (they often neglect the impact of battery chemistry[59-61]); geographical and/or temporal temperature variance (which impacts battery degradation); and, driving intensity by vehicle type in different

countries/regions (which constrains the total capacity available during the day). These factors determine the technical grid storage capacity. Additionally, consumer participation in the vehicle-to-grid market and in the second-use market impacts the actual grid storage capacity[54], which is important but rarely quantified.

Here we link three models and databases to provide an estimate of the grid storage capacity of EV batteries globally by 2050 for both vehicle-to-grid applications and EoL opportunities (see Methods and Supplementary Fig. 5.1). We cover the main EV battery markets (China, India, EU, and US) explicitly, and combine other markets in a Rest of the World region (RoW). The first model is a dynamic battery stock model, which estimates the future battery demand in each region as part of transport fleets per region (Supplementary Fig. 5.2). The model incorporates two EV fleet development scenarios from the IEA (International Energy Agency), the stated policy scenario (STEP) and the sustainable development scenario (SD). The scenarios include two battery chemistry variants to encompass different technological paths: one which is dominated by Lithium nickel cobalt oxides (NCX, representing NMC or NCA with X denoting manganese or aluminum) and another dominated by Lithium-ion phosphate or (LFP). The second model assesses EV use and provides potential EV driving and charging behavior for small, mid, and large size BEV (battery electric vehicles) and PHEV (plug-in hybrid electric vehicles) based on daily driving distance distributions for different regions (Supplementary Fig. 5.3, Supplementary Fig. 5.4, and Supplementary Fig. 5.5). The third model combines information from the other models on EV use behavior, battery chemistry, and temperature in each region with the latest battery degradation data for NCX[59,60,191] and LFP[61] chemistries to account for region- and chemistry-specific battery degradation (Supplementary Fig. 5.6).

We first analyze the technical capacity for short-term grid storage from vehicle-to-grid and second-use. We choose the industry standard, 4-hour storage capacity on a daily basis, as EV batteries are unsuitable for longer-term, seasonal storage due to their chemistries and use cases. We further analyze the impact of different participation rates of EV owners in vehicle-to-grid as well as the impact of different second-use participation rates of retired EV batteries in second-use business (see methods for further details). Finally, we compare these potentials against several scenarios for future storage requirements from the literature.

Short-term grid storage demand scenarios. Future electricity grids will require a

combination of short-term energy storage (discharge duration of several hours throughout a day, such as battery energy storage) and long-term storage (discharge duration of days, months, and seasons, such as pumped hydro storage technologies). We focus here on short-term energy storage since this accounts for the majority of the required power storage capacity[192]. Short-term energy storage demand is defined as a typical 4-hour storage system, referring to the ability for the storage system to operate at a capacity where the maximum power delivered from that storage over time can be maintained for 4 hours. For example, the 4-hour storage capacity of batteries that together deliver a maximum of 0.25 GW until depletion will be 1-Gigawatt hour[193] (GWh). The short-term storage capacity and power capacity are defined based on a typical 1-time equivalent full charging/discharge cycle per day (amounting to 4 hours of cumulative maximum discharge power per day).

We compare our results with storage requirements reported in the IRENA (International Renewable Energy Agency) Planned Energy Scenario (with a warming "likely 2.5°C" in the second half of this century) and the Transforming Energy Scenario (with a warming of "well below 2°C" in the second half of this century)[2]. We also compare our results with storage capacity requirements summarized by the influential Storage Lab for both conservative and optimistic scenarios[194]. Both Storage Lab scenarios result in a warming of "well below 2°C" by 2100, but differ in the role of grid storage in the energy system. For further details on these scenarios see Supplementary Table 5.1. These scenarios lead to short-term grid storage demands of 3.4, 9, 8.8, 19.2 TWh respectively, or 10 TWh on average by 2050. With the 4 hours delivery period, this implies that a power capacity demand is within a range of 850-4800 GW or 2500 GW on average by 2050.

5.2 Methods

5.2.1 Model overview

We develop an integrated model to quantify the future EV battery capacity available for grid storage, including both vehicle-to-grid and second-use (see Supplementary Fig. 5.1 for an overall schematic). The integrated model includes three sub-models:

1) A dynamic battery stock model[7] to estimate total future EV battery stock and the retired batteries at vehicle EoL. This model considers EV fleet (*i.e.*, battery stock) development and EV lifespan distribution (Supplementary Fig. 5.2), as

well as future chemistry development.

2) An EV use model which includes behavioral factors such as EV driving cycle and charging behavior (changing power, time, and frequency), based on daily driving distance data for small/mid-size/large BEVs and PHEVs (Supplementary Fig. 5.3, Supplementary Fig. 5.4, and Supplementary Fig. 5.5).

3) A battery degradation model based on the latest battery degradation test data, to estimate battery capacity fading over time under different EV use, battery chemistry, and temperature conditions (Supplementary Fig. 5.6).

5.2.2 Dynamic battery stock model

We build on results and methods from a previous study[7] where we built a global dynamic battery stock model to quantify the stock and flows of EV batteries. We model future EV fleet development (*i.e.*, battery stock) until 2050. We determine the retired battery availability based on battery stock development and EV lifespan distribution (which is assumed to determine the time when EV batteries are retired). Battery degradation does affect the technical performance (such as driving distance capability) of EVs, thus influencing consumers' choice of time when EVs come into EoL. Here, for model simplicity, we assume batteries will be retired only when EVs come into EoL. While for EV battery capacity, we use an average capacity of 33, 66, and 100 kWh for small/mid-size/large BEVs, and 21, 10, and 15 kWh for small/mid-size/large PHEVs.

EV fleet scenarios. We use two EV fleet scenarios until 2030 from the IEA: the stated policies (STEP) scenario and the sustainable development (SD) scenario. We further extend these two scenarios to 2050 based on a review of EV projections until 2050. We use the EV fleet share across 5 main EV markets (China, India, EU, US, and RoW) from the IEA until 2030, and keep the EV fleet share by countries/regions in 2030-2050 the same as the year 2030 due to lack of reliable data after 2030 (see Supplementary Data for EV fleet scenarios by countries/regions). Further, we include 56 cities in China, 9 cities in India, 32 cities in EU, 53 cities in US, and 9 cities in RoW. We compile future EV sales share among 159 cities globally in STEP scenario and SD scenario based on future EV fleet projections by counties/regions from the IEA[195] and other data sources[196,197] (see Supplementary Data).

Battery chemistry scenarios. We consider battery market shares by chemistry based on the market share projections until 2030 from Avicenne Energy[198] and potential trends until 2050[80,81,83]. Two battery chemistry scenarios are developed, including a

Lithium Nickel Cobalt Manganese Oxide and Lithium Nickel Cobalt Aluminum Oxide battery dominated scenario or NCX scenario (with X representing Manganese or Aluminum), and a Lithium Iron Phosphate battery dominated scenario or LFP scenario. The detailed battery market shares by chemistry in two scenarios are discussed in[7].

5.2.3 EV use model

Daily driving distance (DDD). We explore the EV driving behavior based on DDD distributions. We build historical EU DDD distributions for small/mid-size/large BEVs/PHEVs models based on data from Spritmonitor.de[199], which has been widely used in literatures[200,201]. We exclude the DDD less than 5 km from the dataset. By comparing various DDDs in multiples of EV range, we classify 5 DDD classes to formulate driving intensity and charging behavior. These 5 classes are divided between 0% of the EV range to 200% of the EV range (*i.e.*, a DDD twice the range of the EV) with intervals of 0-25%, 25-33%, 33-50%, 50-100%, 100-200%. We use the mean DDD of each class for calculations. Further, we compile future DDD in different countries/regions (Supplementary Fig. 5.7, Supplementary Fig. 5.8, Supplementary Fig. 5.9, and Supplementary Fig. 5.10) by assuming the future DDD is proportional to the future energy consumption per vehicle. We calculate future energy consumption per vehicle in different countries/regions based on the IEA's projection on future EV fleet size and associated energy consumption until 2030[195].

EV driving cycle. We assume two commuting trips between home and working place per day on weekdays and two entertaining trips on weekends for all countries/regions. Each trip distance is half of DDD. According to the required trip distance, we compile the driving cycle of each trip (speed versus time) based on the standard US combined driving cycle (*i.e.*, 55% city driving and 45% highway driving, see details in Supplementary Fig. 5.4 and Supplementary Fig. 5.5, and Supplementary Note 5.1).

EV charging. Charging behavior may be affected by charging infrastructure, amongst others, on-board EV charger, consumer preferences. We assume an immediate and slow home charging at constant charging power to full charge for all EV sizes and types because home charging is the major charging way (see Supplementary Data). We assume the home charging power as 1.92, 6.6, 22, and 1.92 kW for small, mid-size, large BEV, and PHEV, respectively[202]. We assume that due to high costs and limited utility no consumers will install higher power charging infrastructure at home. We

further anticipate the charging behaviors in terms of changing frequency by comparing the various DDDs in multiples of the EV range. As driving intensity increases, the higher charging frequency is assumed for 5 DDD classes (1x every four days, 1x every three days, 1x every two days, 1x each day, and 2x every day respectively). For example, if the DDD of mid-size BEV (with a 312 km EV range) increases from 75 km to 625 km, and the battery needs to be charged more frequently from 1 time per four days to 2 times per day.

Battery State-of-Charge (SoC) profile. We calculate the EV battery SoC second by second under three EV states: driving, parking and charging, and parking without charging. For battery SoC during driving, we use FASTSim model[202] developed by NREL to calculate EV battery SoC second-by-second based on inputs of the EV driving cycle, EV configurations, and battery performance parameters (specific energy and battery capacity). We select one representative EV model from the FASTSim model[202] for each EV size and type as EV configuration (Supplementary Table 5.2), and NCM622 as representative chemistry for all EV types; because it was found that EV configurations and battery performance parameters (such as specific energy) had small effects on the resulting battery SoC simulations. For battery SoC during charging, we assume the battery SoC increases linearly under a constant charging power with a 90% charging efficiency[203]. For battery SoC during parking without charging, the battery SoC decreases due to self-charging. A typical self-discharging rate of 5% per month is assumed for lithium-ion battery[204]. Note that for the sake of battery safety, a portion of battery capacity is unusable (15% for BEVs and 30% for PHEVs based on the BatPac model[205]), therefor we assume the usable battery SoC range as 5%-90% for BEV battery and 15%-85% for PHEV battery.

Battery temperature. The battery temperature depends on the heat generation from chemical reactions inside batteries, amongst others, ambient temperature and environment (such as solar power radiation), battery management system (air or liquid cooling system to control battery temperature). The temperature can also vary from cell to cell, module to module, and component to component in the battery pack. The modelling of battery temperature is complicated and out of scope of this study. Here we use city ambient temperature to represent battery temperature, which is then used to battery degradation. Here, we use the monthly average temperature of total 159 cities to capture the effects of geographic and temporal temperature variance on

battery degradation. The temperature data is collected from[206-209], which can be found in Supplementary Data.

5.2.4 Battery degradation model

Degradation model development. Battery degradation is crucially important for determining EV battery capacity both in use and for second life applications, but there are still many open research questions surrounding the importance of EV driving habits, charging behavior, and battery chemistries on capacity development[210]. Degradation model approaches include physics based degradation models[211] as well as machine learning models[75,212] though there is no agreed-upon best practice[213]. Here, to balance the complexity and accuracy of battery degradation model, we develop a semi-empirical battery degradation model based on method from[61]. The model considers both calendar life and cycle life aging (equation (1)), assuming a square-root dependence on time for calendar life (degradation rates depend on temperature and SoC, see equation (2)) and a linear dependence on energy throughput for cycle life (degradation rates depend on temperature, Depth-of-Discharge (DoD), and Current rate (C_{rate}) see equation (3)).

$$q = 1 - q_{Loss,Calendar} - q_{Loss,Cycling} \tag{1}$$

$$q_{Loss,Calendar} = k_{Cal} \cdot exp\left(\frac{-E_a}{RT}\left(\frac{1}{T} - \frac{1}{T_{ref}}\right)\right) \cdot exp\left(\frac{\alpha F}{R}\left(\frac{U_a}{T} - \frac{U_{a,ref}}{T_{ref}}\right)\right) \cdot \sqrt{t} \tag{2}$$

$$q_{Loss,Cycling} = k_{Cyc} \cdot (A \cdot DOD + B) \cdot (C \cdot C_{rate} + D) \cdot \left(E \cdot \left(T - T_{ref}\right)^2 + F\right) \cdot EFC \tag{3}$$

where q is the relative battery degradation, $q_{Loss,Calendar}$ is the relative calendar life degradation, $q_{Loss,Cycling}$ is the relative cycling life degradation, T is temperature, t is time (unit: days), EFC is equivalent full cycles. Note R is the universal gas constant (8.3144598 J/mol·K), T_{ref} is the reference temperature (298.15 K), F is Faraday constant (96485 C/mol), k_{Cal} (unit: $days^{0.5}$), E_a (unit: J/mol·K), and α (no unit) are fitting parameters for calendar life degradation, and k_{Cyc} (unit: EFC^{-1}). A, B, C, and D (no units) are fitting parameters for cycling life degradation. The value of the anode-to-reference potential, U_a (unit: V), is calculated from the storage SoC using equations (4) and (5)[214].

$$\begin{aligned} U_a(x_a) = {} & 0.6379 + 0.5416 \cdot exp(-305.5309 \cdot x_a) + 0.044\, tanh\left(-\frac{x_a - 0.1958}{0.1088}\right) \\ & -0.1978\, tanh\left(\frac{x_a - 1.0571}{0.0854}\right) - 0.6875\, tanh\left(\frac{x_a + 0.0117}{0.0529}\right) - 0.0175\, tanh\left(\frac{x_a - 0.5692}{0.0875}\right) \end{aligned} \tag{4}$$

where x_a, which represents the lithiation fraction of the graphite, is a simple linear function of the SoC[215]:

$$x_a(SOC) = x_{a,0} + SOC \cdot (x_{a,100} - x_{a,0}), x_{a,0} = 0.0085, x_{a,100} = 0.78 \quad (5)$$

where $x_{a,0}$ is the lithiation fraction of the graphite at 0% SoC and $x_{a,100}$ is the lithiation fraction of the graphite at 100% SoC.

To obtain these fitting parameters, we collect publicly available battery degradation data, including calendar life aging and cycle life aging, for NCM[61] and LFP[59,60,191] chemistry. These data sets represent state-of-the-art lifetime performance for each chemistry; the LFP cells shown reach between 5000 and 8000 equivalent full cycles before reaching 80% remaining capacity, 4000~5000 equivalent full cycles for NCM cells. This experimental data was then fit with the semi-empirical model equations (1), (2), and (3) using a non-linear least squares solver in MATLAB. The NCM model has no C_{rate} dependence, due to lack of data in the aging data set, so the parameters C and D are simply set at 0 and 1. We first fit the calendar fade data with the time-dependent portion of the model ($q_{Loss,Calendar}$, parameters k_{Cal}, E_a, and α); the parameter α is bounded between -1 and 1, with other parameters unbounded. The parameters for the cycling fade (A, B, C, and D) are optimized on the cycling aging data. For both LFP and NCM, the raw cycling fade data was processed prior to optimizing a model based on expert judgement. For LFP, only cells with linear fade trajectories and data for at least 5000 EFCs were used for model optimization. For NCM, only data after 200 EFC at T > 5 °C and data at q < 0.85 at T < 5 °C was used for optimization of the NCM cycling model parameters. The optimized parameters for the LFP and NCM degradation models are shown in Supplementary Table 5.3. Fitting results are shown in Supplementary Fig. 5.11 and degradation rates are shown in Supplementary Fig. 5.12.

Note that we assume NCA battery has the same degradation patterns as NCM battery due to a lack of state-of-the-art open-source data for NCA batteries. Besides cell chemistry, capacity degradation characteristics vary with cell design, manufacturing process, and proprietary additives[210,216], which is out of scope of this study. We use cell degradation patterns to represent battery pack degradation without consideration of cell-to-cell and module-module differences.

Battery degradation under different driving and temperature conditions. For

simulation of the degradation under the EV driving loads (battery SoC evolution over time) and during dynamic temperature changes, the degradation model is reformulated to solve for the degradation occurring during consecutive timesteps[60]. We choose a timestep of 1 day for making SoH updates and update the SoC timeseries for each day by the current SoH. At each timestep, the temperature is the average temperature during the simulation month at cities from different countries/regions. Average SoC, DoD, C_{rate}, and the number of EFCs is extracted from the SoC timeseries. Average SoC refers to the time-averaged value of SoC. DoD is the difference between the maximum and minimum values of SoC. C_{rate} is calculated using the absolute change of SoC per second, and then taking the average of all C_{rates} greater than 0 during the entire timeseries. The number of EFCs is calculated by summing the changes to SoC over the timeseries. Dependence of the expected degradation rate on current SoH is incorporated by calculating a 'virtual time'[60]. The virtual time is found by inverting the calendar degradation equation to solve for time:

$$t_{virtual} = \left(q_{Current} \Big/ k_{Cal} \cdot exp\left(\frac{-E_a}{RT}\left(\frac{1}{T} - \frac{1}{T_{ref}}\right)\right) \cdot exp\left(\frac{\alpha F}{R}\left(\frac{U_a}{T} - \frac{U_{a,ref}}{T_{ref}}\right)\right) \right)^2 \tag{6}$$

The degradation change Δq during any given timestep Δt is then calculated by the following equation:

$$\Delta q = \left(k_{Cal} \cdot exp\left(\frac{-E_a}{RT}\left(\frac{1}{T} - \frac{1}{T_{ref}}\right)\right) \cdot exp\left(\frac{\alpha F}{R}\left(\frac{U_a}{T} - \frac{U_{a,ref}}{T_{ref}}\right)\right) \Big/ 2 \cdot \sqrt{t_{virtual} + \Delta t} \right) \cdot \Delta t + k_{Cyc} \cdot (A \cdot DOD + B) \cdot (C \cdot C_{rate} + D) \cdot \left(E \cdot \left(T - T_{ref}\right)^2 + F\right) \cdot \Delta EFC \tag{7}$$

For cycling fade, the virtual EFC does not need to be calculated, as the degradation rate is constant with respect to the change of EFC during any given timestep. This reformulation of the degradation model captures the path-dependent degradation observed in real-world battery use. See Supplementary Note 5.2 for modelled battery degradation for NCM and LFP.

5.2.5 Available capacity from EV batteries

Battery capacity during use and when retired from EV. Vehicle EoL does not necessarily correspond to battery EoL. With technological improvements in battery

reliability and durability, many batteries in EoL vehicles may still have years of useful life at the end of vehicle end of life. Vehicle battery EoL is usually as defined the time at which remaining battery capacity is between 70%-80% of the original capacity[15]. We assume an EV lifespan distribution, as in our previous work[7] to account for EoL of EV. In our modelling approach, the vehicle lifespan distribution determines when batteries are not used in EVs any more (*i.e.*, retired batteries). Retired batteries may have quite different capacity under different use conditions. When vehicles reach EoL due to consumer choices or other issues before the battery pack reaches 70% relative capacity, retired batteries will still have over 70% relative SoH and are assumed to be used in a second-life application. When battery pack reaches 70% relative SoH before a vehicle reaches its EoL, we assume that batteries may still be used in EVs for low distances-driving. Retired batteries from such vehicles will have lower than 70% relative SoH and are assumed to be recycled rather than for a second-use. We assume any battery with a relative SoH lower than 60% is recycled and removed from potential grid storage capacity[217]. However, even batteries with a relative SoH of 60%-70% have a limited economic value and can have relatively high safety risks. (methods)[218].

Vehicle-to-grid capacity. We define technical vehicle-to-grid capacity as the availability of EV battery stock capacity for vehicle-to-grid application, considering the capacity reserved for EV driving, the capacity of PHEVs that will not participate in vehicle-to-grid due to low capacity, and capacity fade due to battery degradation. We further define the actual vehicle-to-grid capacity as the availability of technical vehicle-to-grid capacity for the grid under different consumer participation rates in the vehicle-to-grid business. Results focus on investigating under which participation rate can actual vehicle-to-grid capacity meet grid storage demand.

Second-use capacity. The technical second-use capacity is defined as the retired battery capacity that can be repurposed (*i.e.*, retired batteries with over 70% relative SoH). We further investigate actual second-use capacity under different market participation rates (*i.e.*, not all retired batteries will participate in second-use). The results are intended to determine the required market participation rate for the actual second-use capacity to meet grid storage demand.

5.3 Results

Total technical capacity. We define technical capacity as the total cumulative available

EV battery capacity in use and in second use at a specific time, taking into account battery degradation and the capacity needed to meet driving demand. Globally, the SD scenario sees total technical capacity twice that of the STEP scenario due to the larger fleet size (see Supplementary Fig. 5.13 and Note 1). The LFP scenario sees a higher cumulative capacity than NCX due to the lower degradation of LFP across most countries/regions (see Supplementary Data for a comparison of LFP and NCM battery degradation). As shown in Fig. 5.1, the highest total technical capacity is provided in the SD-LFP scenario that is 48% higher by 2030 and 91% higher by 2050 than in the STEP-NCX scenario (respectively 3.8 TWh and 2.6 TWh in 2030 and 32 TWh and 62 TWh in 2050).

Under all scenarios, the cumulative vehicle-to-grid and second use capacity will grow dramatically, by a factor of 13-16 between 2030 and 2050. Putting this cumulative technical capacity into perspective against future demand for grid storage we find that our estimated growth is expected to increase as fast or even faster than short-term grid storage capacity demand in several projections[56,194] (Fig. 5.1). Technical vehicle-to-grid capacity or second-use capacity are each, on their own, sufficient to meet the short-term grid storage capacity demand of 3.4-19.2 TWh by 2050. This is also true on a regional basis where technical EV capacity meets regional grid storage capacity demand (see Supplementary Fig. 5.14).

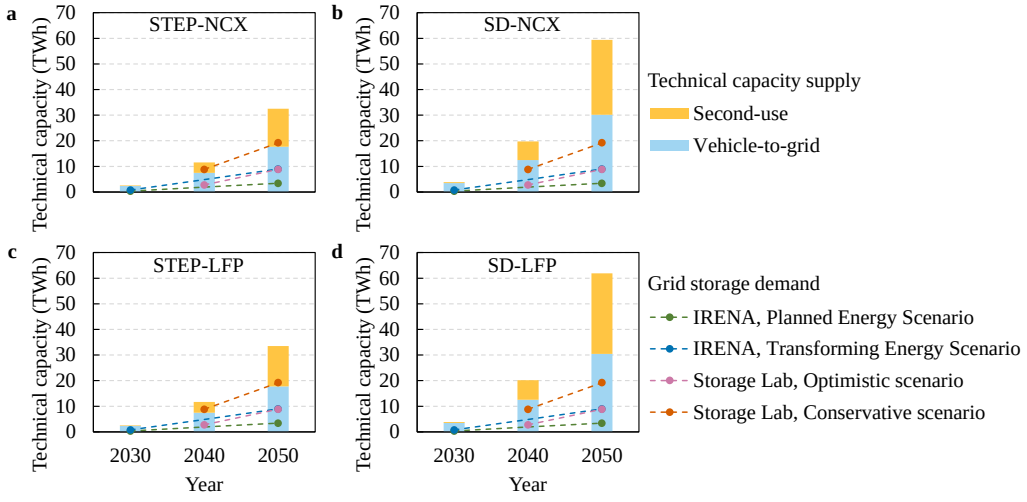

Fig. 5.1: Total technical capacity for EV batteries and comparison to grid storage demand. a STEP-

NCX scenario. **b** SD-NCX scenario. **c** STEP-LFP scenario. **d** SD-LFP scenario. The storage requirements of grids are 0.37-0.745 TWh in 2030 based on the IRENA[56], and that of 2050 from both IRENA and Storage Lab[194] (see details in Supplementary Table 5.1).

Factors limiting total technical capacity.

Vehicle-to-grid.

Examining the vehicle-to-grid opportunity alone, without considering second use, we find that 21%-26% of the global theoretical battery stock capacity (*i.e.*, on-board EV battery capacity of the entire EV fleet without considering battery degradation) could be available for vehicle-to-grid services by 2050 (Fig. 5.2a). The most important limiting factor is the battery capacity required to meet consumer driving demands[195,199] which can limit the technically available stock capacity by 57%-63%. PHEVs, which make up around 11% of the theoretical stock capacity in 2050, are not considered for vehicle-to-grid as they have a low storage potential due to low capacities. On average, just 5% of the theoretical stock capacity is lost due to battery degradation by 2050. These losses vary between 7% in India and 4% in RoW due to differences in regional factors such as use conditions and temperature (see regional results in Supplementary Fig. 5.15). Overall, taking these factors into account yields a technical vehicle-to-grid capacity of roughly 18-30 TWh by 2050 (see Fig. 5.2).

However, there are other factors that may limit actual available storage capacity. The vehicle-to-grid participation rate is the most important of these. That is, not all EV consumers will necessarily participate in the market. The impact of different participation rates, defined as the percentage of the technical vehicle to grid capacity actually connected to the grid, is shown in Fig. 5.2b. To satisfy the short-term storage demand of 10 TWh in 2050, participation rates of 38% and 20% are required for the STEP-NCX and SD-NCX scenarios, respectively. In practice, it is likely that EVs with high battery capacities and low degradation will be used for providing vehicle-to-grid services since these will provide the highest revenue for EV owners[219] (the full battery capacity distributions by 2050 across countries/regions is available in Supplementary Fig. 5.16, Supplementary Fig. 5.17, Supplementary Fig. 5.18, Supplementary Fig. 5.19, and Supplementary Fig. 5.20).

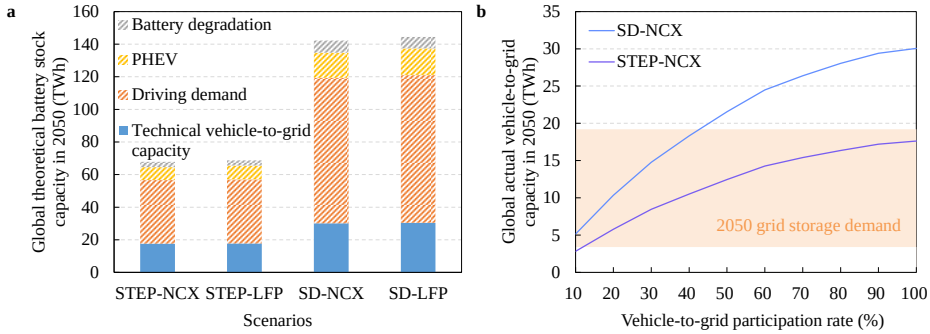

Fig. 5.2: Global available vehicle-to-grid capacity in 2050. a Technical vehicle-to-grid capacity. Hatched bars indicate the capacity limits due to key factors and blue bars the technical vehicle-to-grid capacity. **b** Actual vehicle-to-grid capacity as a function of participation rates. Results are shown for the STEP-NCX and the SD-NCX scenarios with a comparison to the range of storage demand computed by IRENA and Storage Lab models in 2050 (orange shading). Please see Supplementary Fig. 5.21 for global actual vehicle-to-grid capacity under the STEP-LFP and the SD-LFP scenarios, which shows similar results as STEP-NCX and SD-NCX scenarios. Supplementary Fig. 5.22, Supplementary Fig. 5.23, Supplementary Fig. 5.24, and Supplementary Fig. 5.25 for regional actual vehicle-to-grid capacity.

Second-use.

Over time EV batteries degrade so far that they cannot be used to power vehicles[7]. This is typically when the battery relative State of Health (SoH), defined as actual capacity as percentage of original capacity, has reached 70%-80%[15], although the relative SoH could fall even lower if a consumer is willing to accept relatively poor battery health and shorter ranges[119]. Given their high value, size and end of life regulations in many countries we assume all retired batteries will be collected[17]. Once collected, batteries are health tested to determine if the retired EV battery can be used in a less critical second-use application, or if the battery must be recycled[220].

Given the technical and economic feasibility of retired batteries for a second-use[218], we consider batteries with an SoH of 70% and higher only for second-use (this threshold is often assumed as a technically and economically feasible value for second-use businesses[218]). Using this criterion, we find that for all scenarios between 2030 and 2050 74% of the retired NCX batteries can be repurposed for second-use globally (*i.e.*, repurposing percentage), while 26% goes to recycling by 2050. Regional differences can be significant due to the impact of temperature on NCX battery degradation (see Supplementary Fig. 5.26 and Supplementary Data). In contrast, virtually all LFP retired

batteries can be repurposed.

Business models are still developing, and repurposing is highly dependent on the technical specifications and market requirements of second-use applications[221]. Since battery disassembly is costly[218], battery repurposing will likely happen on the pack level instead of modules and cell level. Repurposing will consist mainly of rebalancing and reconnecting the retired battery packs. There is no strong technical reason to model a capacity difference before and after the repurposing processes.

For these assumptions, 2.1-4.8 TWh of retired batteries are estimated to become available as annual technical second-use capacity globally in 2050, as shown in Fig. 5.3a. The cumulative technical second-use capacity is expected to reach 14.8-31.5 TWh by 2050 when using a 10-year second-use life scenario[222] (Fig. 5.3b). The actual second second-use lifespan is uncertain due to uncertainties surrounding the retired battery SoH, use conditions, *etc*. Another uncertainty is the further battery degradation during secondary use, which is difficult to model due to complicated degradation mechanisms of retired batteries[223]. Further research into degradation and second-use life span is required to improve estimates of technical second-use capacity.

Similar to estimates for actual vehicle-to-grid capacity, the second use participation rate determines which percentage of the technical second-use capacity is actually available and connected to the grid. To meet the requirement of a 10 TWh short-term storage capacity in the STEP-NCX scenario (14.8 TWh technical capacity) a participation rate 68% is required, while in the SD-LFP scenario (31.5 TWh technical capacity) a participation rate of 32% is needed.

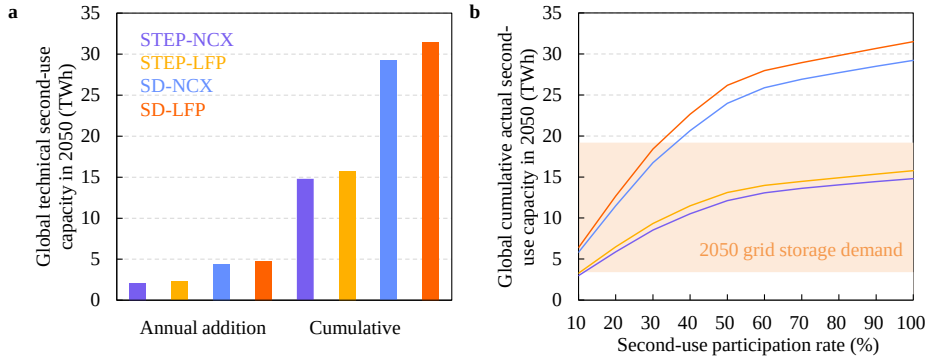

Fig. 5.3: Global available second-use capacity in 2050. a Annual addition and cumulative technical capacity in 2050. Capacity refers to the technically available capacity considering battery degradation, or maximum theoretical potential second-use capacity without considering the battery second-use participation rate. **b** Impacts of second-use participation rate on cumulative actual second-use capacity and a comparison to storage demand in 2050 (orange shading). See Supplementary Fig. 5.27, Supplementary Fig. 5.28, Supplementary Fig. 5.29, and Supplementary Fig. 5.30 for regional actual second-use capacity.

Combining vehicle-to-grid and second-use participation rates.

As we describe above, the global technical capacity for short-term grid storage of EV batteries grows rapidly in all scenarios. However, the actual available capacity depends strongly on the vehicle-to-grid and second-use participation rates. We show the actual available capacity as a function of these participation rates in Fig. 5.4 for the STEP-NCX scenario (please see Supplementary Fig. 5.31, Supplementary Fig. 5.32, and Supplementary Fig. 5.33 for other scenarios). If 50% participation rates can be realized for both vehicle-to-grid and second-use, the combined actual available capacity is 25-48 TWh by 2050, far above requirements estimated from the literature. Changes in vehicle-to-grid participation rates of 23%-96%[224,225] could influence this actual available capacity in 2050 by as much as -24% to +21%. When second use participation rates vary 10%-100%, the actual available capacity varies between -41% and 12%. Taken together, vehicle-to-grid participation rate and second use participation rate could alter the actual available capacity in 2050 by -61% to +32%.

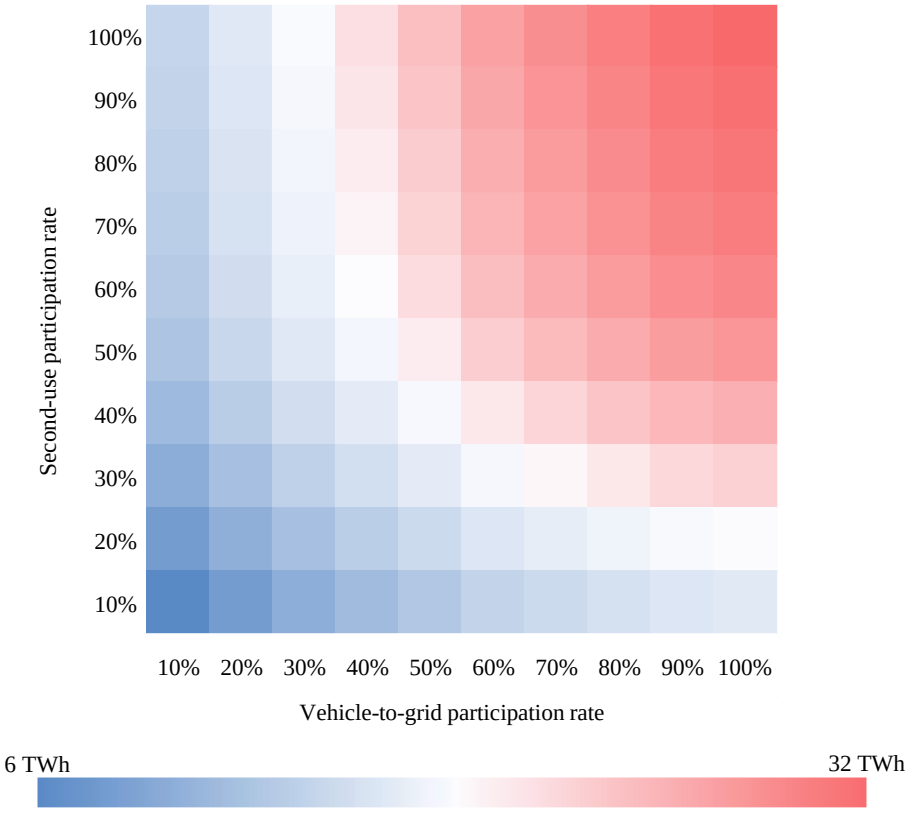

Fig. 5.4: Total actual available capacity under various conditions in STEP-NCX scenario in 2050. Blue, white, and red colors depict minimum, average, and maximum values. See Supplementary Fig. 5.31, Supplementary Fig. 5.32, and Supplementary Fig. 5.33 for other scenarios.

5.4 Discussion

Previous research has suggested that large EV fleets could exert additional stress on grid stability (*e.g.*, if the majority of EVs are charged at grid peak time)[226]. Our findings, from a different perspective, show EV batteries could promote electricity grid stability via storage solutions from vehicle-to-grid and second-use applications. We estimate a total technical capacity of 32-62 TWh by 2050. This is significantly higher as the 3.4-19.2 TWh (10 TWh on average) as required by 2050 in IRENA and Storage lab scenarios.

The actual available capacity depends on participation rates for vehicle-to-grid and second use. Participation rates may vary regionally depending on future market

incentives and infrastructure along with other factors[227]. However, we show how EV batteries in primary and secondary use could provide the 10 TWh short-term grid storage capacity required in the IRENA and Storage Lab scenarios by 2050. The STEP-NCX scenario presented in Fig. 5.4 has the lowest technical capacity (32 TWh compared to 62 TWh in the SD-LFP scenario) which already easily meets requirements at participation rates of 40%-50% for vehicle-to-grid and second-use. At a regional level, even lower participation rates may still contribute significantly to grid stability. Overall, EV batteries could meet short-term grid storage demand by as early as 2030 (if we assume lower requirements from the literature and higher levels of participation). By 2040-2050 storage demands are met across almost all scenarios and even low participation rates. Harnessing this potential will have critical implications for the energy transition and policymakers should be cognizant of the opportunities.

As we include a broader set of limitations for the total opportunity our results are difficult to compare with other literature. Our estimated global EV fleet capacity in 2050 (68-144 TWh) is considerably higher than the estimate from IRENA (7.5-14 TWh)[56]. This is due to the IRENA's very conservative scenarios on future EV fleet size and battery capacity per vehicle. The IRENA scenario also does not consider the availability of EV fleet capacity for grid services. An IEA estimate does not extend beyond 2030[57] but highlights the importance of including battery degradation in analyses, which we include here to project until 2050 (Fig. 5.3).

We note several limitations in our approach that could be improved as data availability improves. For example, while we include battery degradation by using state-of-art data, future battery degradation is highly uncertain and depends on further technological breakthroughs in battery chemistry such as Na-ion, Li-Air, and Li-Sulphur[228] along with developments in battery management systems. Further, while we derived driving behaviour from empirical data, future changes in driving habits are uncertain and dependent on various factors such as EV-related infrastructure. Vehicle chargers increase in power output over time and 50 kW charging is already common across many countries[229]. Frequent fast charging could lead to faster degradation, especially in hot/cold climates[230]. This challenge may be addressed by future technology improvements to battery materials[231], electrode architectures, and optimized synergy of the cell/module/pack system design[169]. A further limitation is that we compare technical and actual available vehicle-to-grid capacity with an average 4-hour storage

requirement as provided in the scenarios by IRENA and Storage Lab. This omits potential differences in storage requirements at shorter time scales (seconds/minutes). Improved modelling and data can overcome this gap. It is however likely that the technical vehicle-to-grid capacity will be sufficient given low vehicle utilization rates of just 5% for many regions[232]. Additionally, development of smart charging infrastructure and grid digitization is likely to provide additional flexibility for matching electricity demand and supply[233].

A final limitation is that we assume that the rated capacity per vehicle remains the same in the future and that a small number of large BEVs might provide large actual vehicle-to-grid capacity (Supplementary Fig. 5.22, Supplementary Fig. 5.23, Supplementary Fig. 5.24, and Supplementary Fig. 5.25). These capacities may change further in the future due to policy incentives, vehicle design, consumer preferences, charging infrastructure, among other factors. Further, the transportation system could see radical and fundamental changes. A significant and rapid shift away from private car use to mass transit, a move to shared electric vehicles, autonomous driving, and the success of battery swap systems[234] could all alter the available capacity via utilization rates and other factors by 2050.

Glossary

Dynamic battery stock model:

EV: electric vehicles.

BEV: battery electric vehicle.

PHEV: plug-in hybrid electric vehicle.

LFP: lithium-iron-phosphate / graphite battery.

NCM: lithium Nickel Cobalt Manganese Oxide / graphite battery.

NCA: lithium Nickel Cobalt Aluminum Oxide / graphite battery.

NCX: NCM and NCA, with X denoting manganese or aluminum.

EV use model:

Ambient temperature: the temperature of the air surrounding the EVs under consideration.

Daily driven distance (DDD): assumed as the mean value of DDD distribution.

State of Charge (SoC): level of charge of a battery relative to its rated capacity, and the units of SoC are percentage points (0% = empty; 100% = full).

$\mathbf{C_{rate}}$: the charge or discharge current divided by the battery's capacity to store an electrical charge. The unit of the $\mathbf{C_{rate}}$ is $hour^{-1}$.

Depth of discharge (DOD): the fraction or percentage of the battery's capacity which is currently removed from the battery with regard to its (fully) charged state.

Equivalent full cycles (EFCs): the charge throughput of partial cycles relative to a full charge/discharge cycle.

Battery degradation model:

Rated capacity: the maximum energy of the battery at the start of life.

Battery degradation: the amount of charge a rechargeable battery can deliver at the rated voltage decreases with use, depending on lots of stress factors: Ambient temperature SoC, Crate, DoD, and EFCs.

Battery capacity: a property of that a battery's maximum capability to store the energy at a given moment in time and conditions, as the battery degradation.

Relative SoH: state of health, is assumed as Battery capacity / Rated capacity.

Vehicle-to-grid model:

Theoretical battery stock capacity: on-board EV battery capacity of total EV fleet, without considering capacity lost due to battery degradation. Theoretical battery stock capacity = Rated capacity per EV * number of total EVs.

Technical vehicle-to-grid capacity: availability of theoretical battery stock capacity for vehicle-to-grid applications, considering driving demand, battery degradation, and PHEV. Technical vehicle-to-grid capacity = Theoretical battery stock capacity – Battery capacity reserved for BEV driving – Battery capacity of PHEV - Battery capacity lost due to battery degradation.

Vehicle-to-grid participation rate: Number of EVs participating in vehicle-to-grid / Number of total EVs.

Actual vehicle-to-grid capacity: availability of technical vehicle-to-grid capacity for vehicle-to-grid applications. Actual vehicle-to-grid capacity = number of EVs participating in vehicle-to-grid * technical vehicle-to-grid capacity per EV.

Second-use model:

Retired battery: battery out of service from first life of EV.

Capacity per retired battery: battery capacity when coming to the end of the first life of EV.

Collection rate per year: number of collected batteries per year / number of retired batteries per year. Number of collected batteries per year = number of repurposed batteries + number of recycled batteries.

Repurposing battery: retired battery that is suitable for electricity storage. The model assumes collected battery with relative SoH above 70% will be repurposed.

Recycled battery: retired battery that is collected for material recycling.

Repurposing rate per year: rate of repurposing batteries in collected batteries. Repurposing rate per year = number of collected batteries with relative SoH above 70% per year / number of collected batteries per year.

Recycling rate per year: rate of recycled batteries in collected batteries. Recycling rate per year = 1- repurposing rate per year.

Technical second-use capacity per year: battery capacity of repurposed batteries per year. Technical second-use capacity per year = number of retired batteries per year * collection rate per year * repurposing rate per year * capacity per retired battery.

Second-use participation rate per year: number of batteries participating in second-use / number of repurposing batteries (or collected batteries with relative SoH above 70%) per year.

Actual second-use capacity per year: availability of technical second-use capacity per year for second-use applications. Actual second-use capacity per year = technical second-use capacity per year * second-use participation rate per year * capacity per retired battery.

5.5 Supplementary information

5.5.1 Model overview

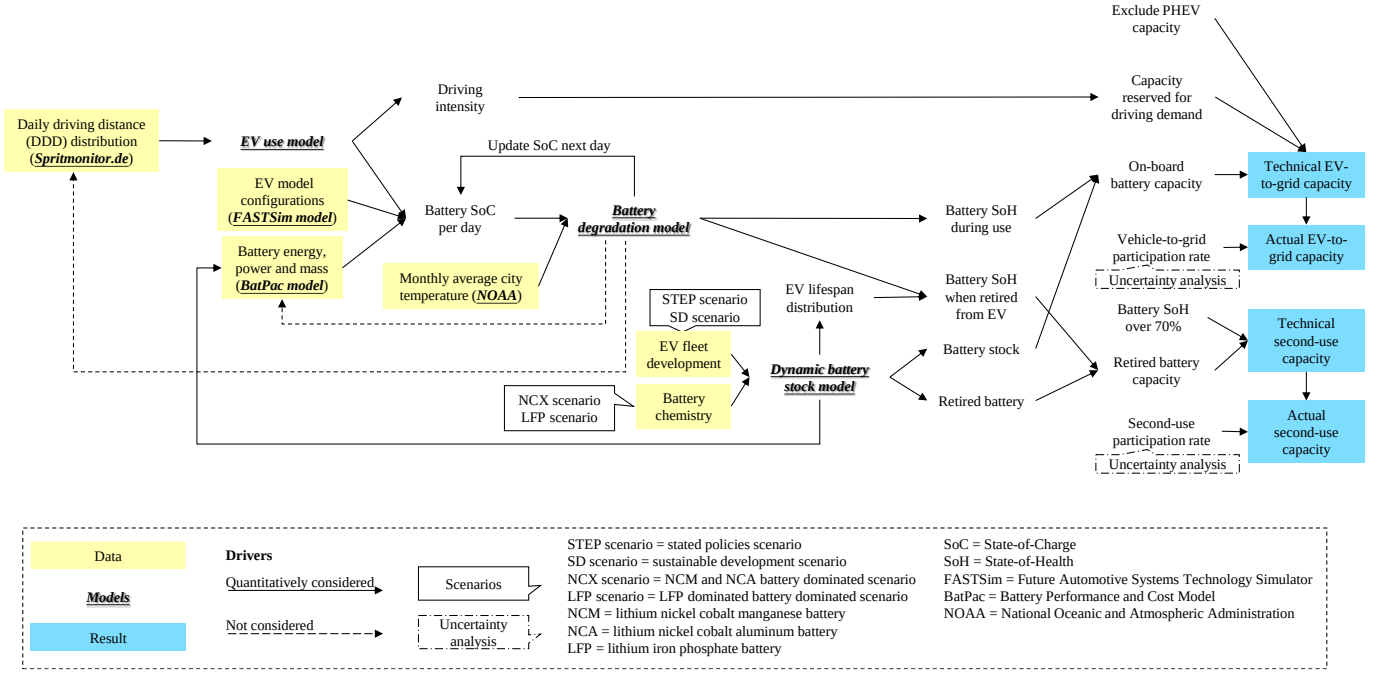

Supplementary Fig. 5.1: Model framework consisting of a dynamic battery stock model, a EV use model, and a battery degradation model.

Dynamic battery stock model

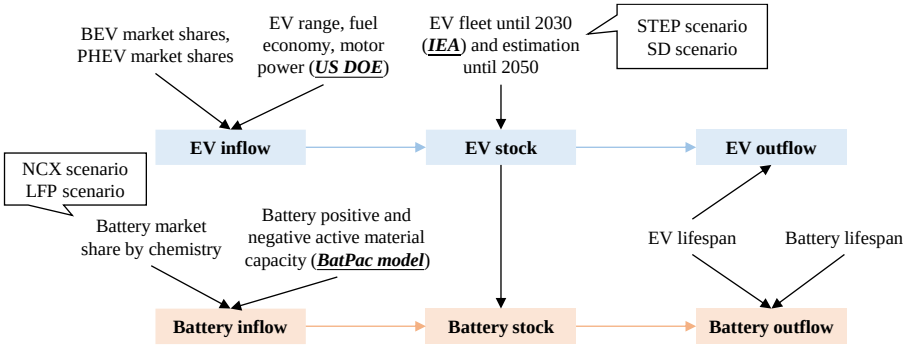

STEP scenario = stated policies scenario
SD scenario = sustainable development scenario
NCX scenario = NCM and NCA battery dominated scenario
LFP scenario = LFP dominated battery dominated scenario
NCM = lithium nickel cobalt manganese battery
NCA = lithium nickel cobalt aluminum battery
LFP = lithium iron phosphate battery

IEA = International Energy Agency
USDOE = U.S. Department of Energy
BatPac = Battery Performance and Cost Model

Supplementary Fig. 5.2: Dynamic battery stock model[7].

EV use model

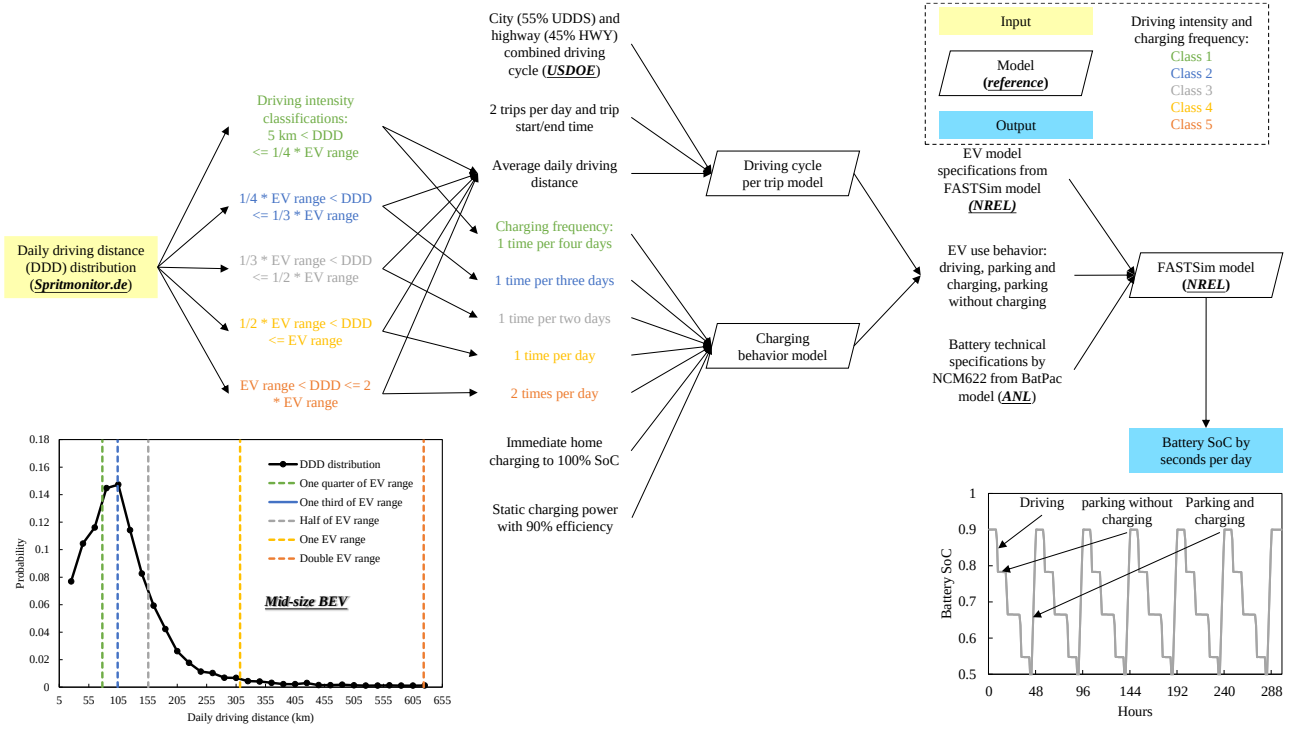

Supplementary Fig. 5.3: EV use model. NREL National Renewable Energy Laboratory. ANL Argonne National Laboratory.

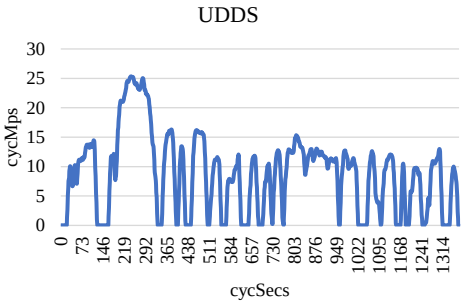

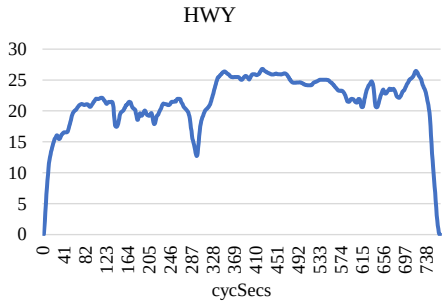

UDDS	
Cumkm	11.99043319
Average speed (m/s)	8.752141014
Time (s)	1369

HWY	
Cumkm	16.50681747
Average speed (m/s)	21.54937007
Time (s)	765

Average daily driving distance = x

Trip distance = 0.5*x

Required UDDS trip distance = 0.55*0.5*x

Required UDDS trip time = ROUND (0.55*0.5*x / UDDS average speed, 0)

Required multiples of UDDS = FLOOR (Required UDDS trip time / UDDS trip time, 1)

Required downsize factor UDDS = Round (UDDS trip time / MOD (Required UDDS trip time / UDDS trip time), 2)

Required HWY trip distance = 0.45*0.5*x

Required HWY trip time = ROUND (0.45*0.5*x / HWY average speed, 0)

Required multiples of HWY = FLOOR (Required HWY trip time / HWY trip time, 1)

Required downsize factor HWY = Round (HWY trip time / MOD (Required HWY trip time / HWY trip time), 2)

For UDDS and HWY, **first scale the resolution from 1s to 0.01 s**. new cycMps (for cycSecs in 0.00-0.49, 0.01s interval) = old cycMps (0); new cycMps (0.50-1.49) = old cycMps (1); new cycMps (1.50-2.49) = old cycMps (2) …

Downsized cycMps (0) = average (new cycMps (0, downsize factor));

Downsized cycMps (1) = average (new cycMps (downsize factor+0.01, 2*downsize factor+0.01)) …

Supplementary Fig. 5.4: EV use model where driving cycle is compiled on trip distance and standard UDDS and HWY driving cycle.

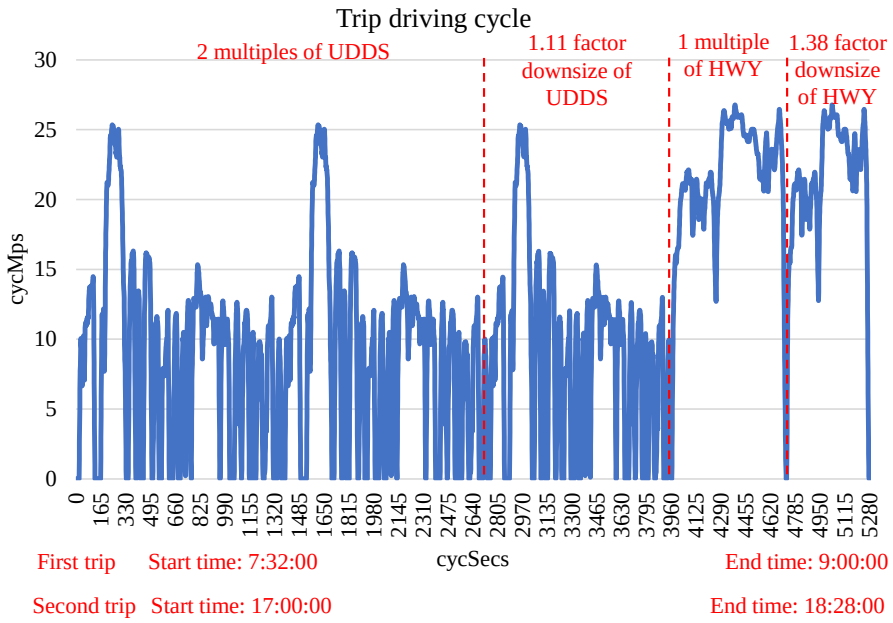

Supplementary Fig. 5.5: EV use model where a drive cycle example is compiled for a mid-size BEV when the daily driving distance is 126.3 km.

Battery degradation model

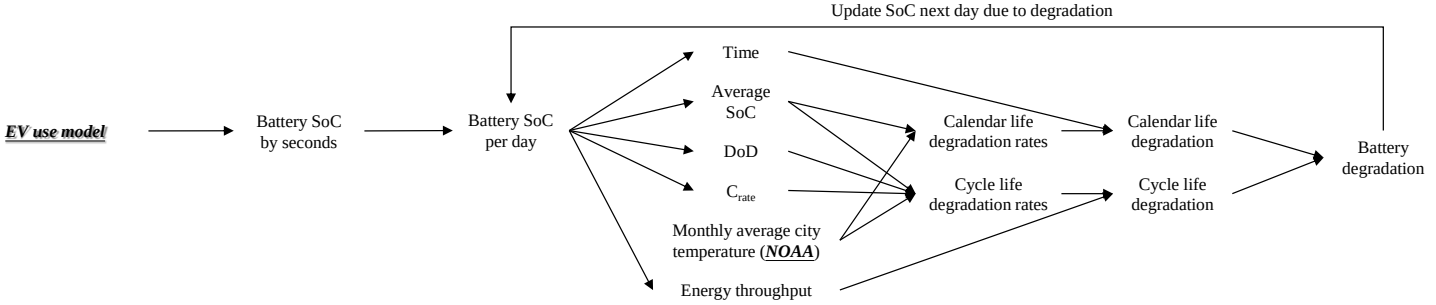

Supplementary Fig. 5.6: Battery degradation model.

5.5.2 Additional Figures and Tables

Supplementary Figures

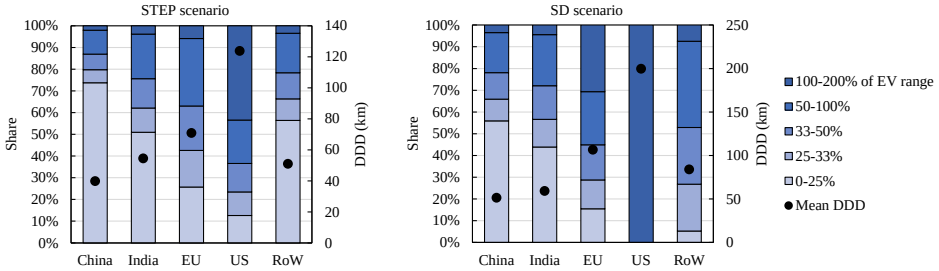

Supplementary Fig. 5.7: Daily driving distance (DDD) distributions for small BEV across counties/regions. The historic DDD distribution for EU is collected from Spritmonitor.de[199]. Combined with the IEA's projection of future EV fleet energy consumption for China, India, EU, US, and RoW[195], we compile the future DDD distributions for countries/regions.

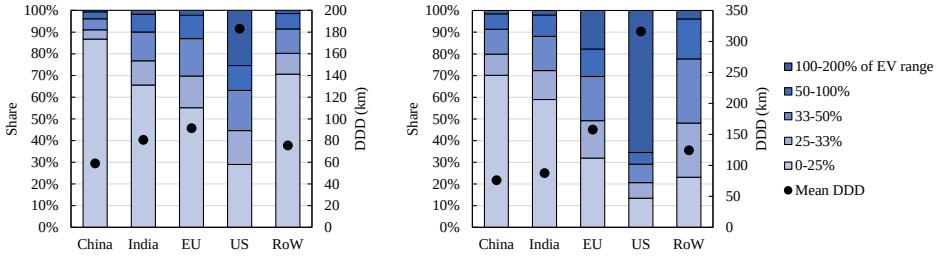

Supplementary Fig. 5.8: Daily driving distance (DDD) distributions for mid-size BEV across counties/regions. The historic DDD distribution for EU is collected from Spritmonitor.de[199]. Combined with the IEA's projection of future EV fleet energy consumption for China, India, EU, US, and RoW[195], we compile the future DDD distributions for countries/regions.

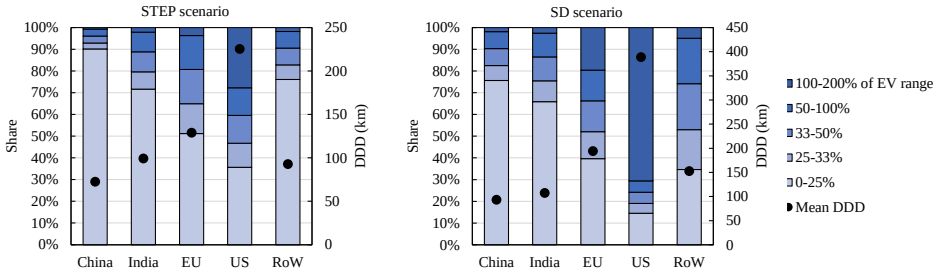

Supplementary Fig. 5.9: Daily driving distance (DDD) distributions for large BEV across

counties/regions. The historic DDD distribution for EU is collected from Spritmonitor.de[199]. Combined with the IEA's projection of future EV fleet energy consumption for China, India, EU, US, and RoW[195], we compile the future DDD distributions for countries/regions.

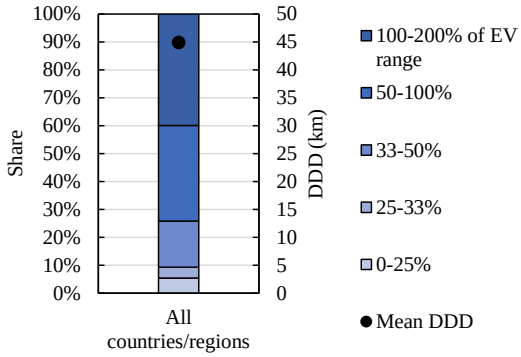

Supplementary Fig. 5.10: Daily driving distance (DDD) distributions assumed for PHEVs for all counties/regions.

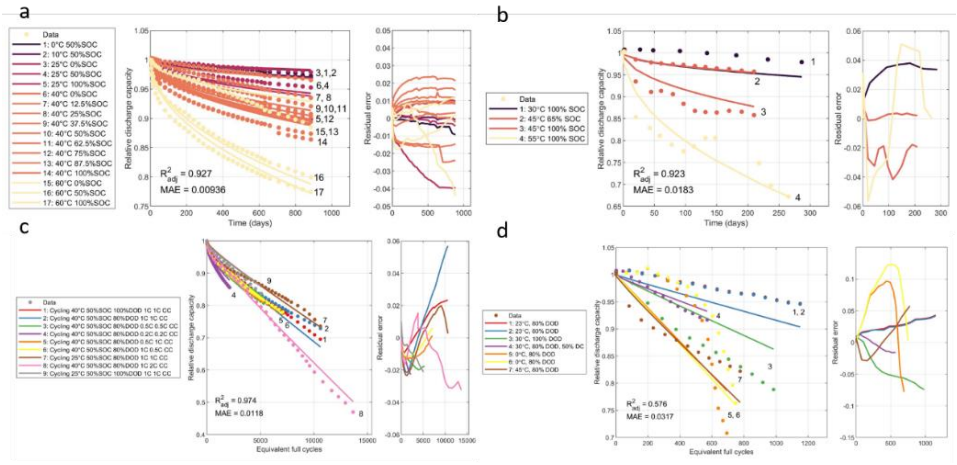

Supplementary Fig. 5.11: Battery degradation model fitting results. a calendar life aging of LFP. **b** calendar life aging of NCM. **c** cycling life aging of LFP. **d** cycling life aging of NCM. Residual errors are plotted to the right of each fit.

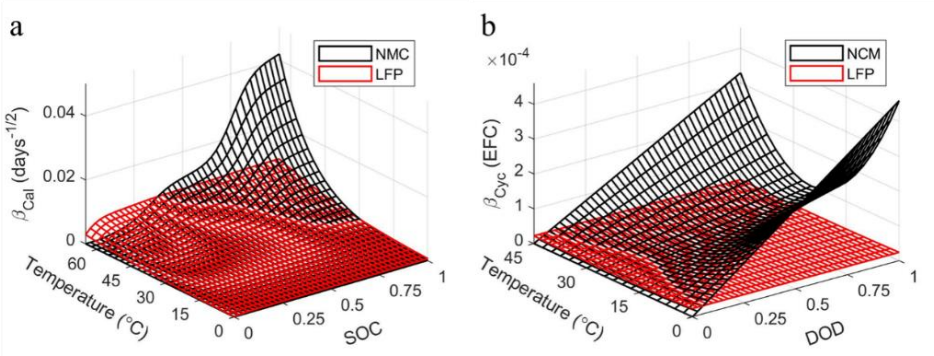

Supplementary Fig. 5.12: LFP and NCM battery degradation rates. a Calendar life degradation rate versus the square-root of time as a function of temperature and SoC (state-of-charge). **b** Cycle life degradation rate versus energy throughput, in units of EFCs (equivalent full cycles), as a function of temperature and DOD (depth-of-discharge).

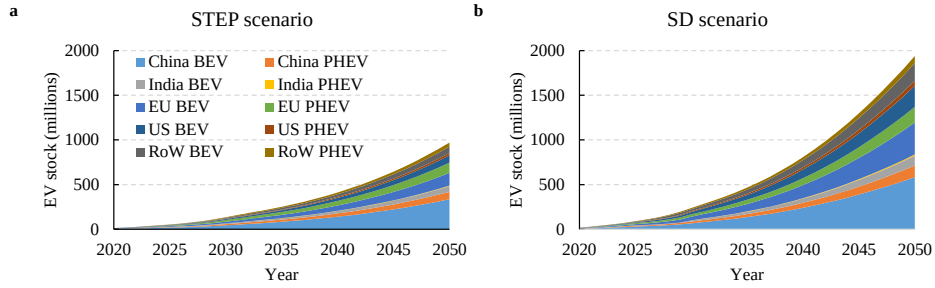

Supplementary Fig. 5.13: Global EV stock development projected until 2050 for STEP and SD fleet scenarios. a STEP scenario. **b** SD scenario. BEV battery electric vehicle, PHEV plug-in hybrid electric vehicle, STEP scenario the Stated Policies scenario, SD scenario Sustainable Development scenario.

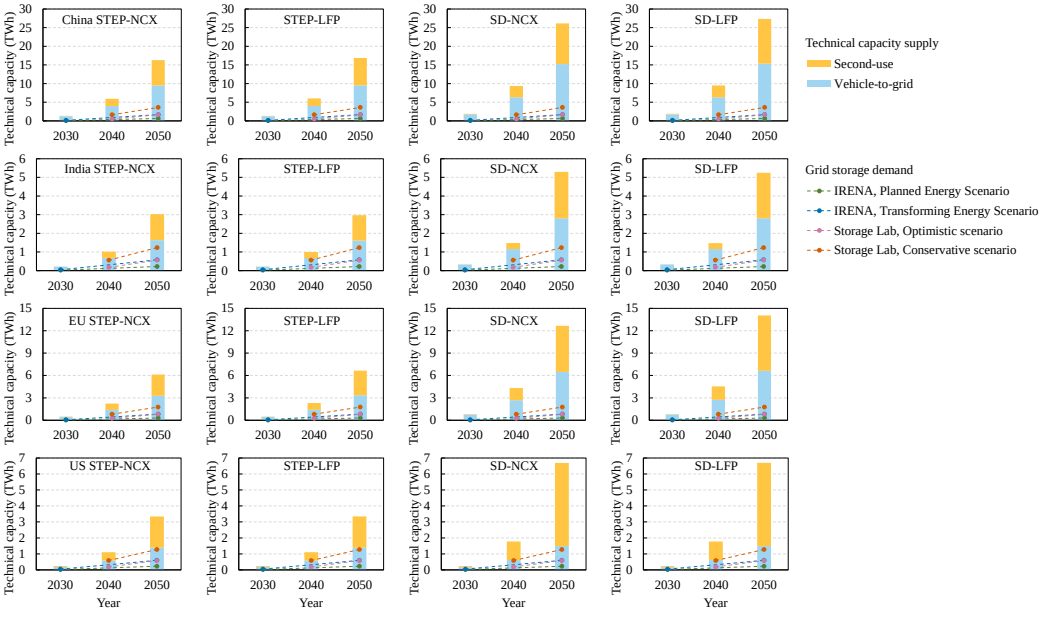

Supplementary Fig. 5.14: Total technical capacity from EV batteries and comparison to grid storage demand in countries and regions. The grid storage demand in countries/regions is estimated based on future peak power demand in countries/regions, where assuming a proportional relationship between grid storage demand and peak power demand for countries/regions is the same as global. Global peak power will increase to 6686 GW in 2030 and 10000 GW in 2050, derived from Storage Lab[194]. China's peak power will increase to 1258 GW in 2030 and 1881 GW in 2050. India's peak power will increase to 430 GW in 2030 and 643 GW in 2050. EU peak power will increase to 616 GW in 2030 and 922 GW in 2050. US peak power will increase to 445 GW in 2030 and 665 GW in 2050. Regional peak demand is from the IEA[57].

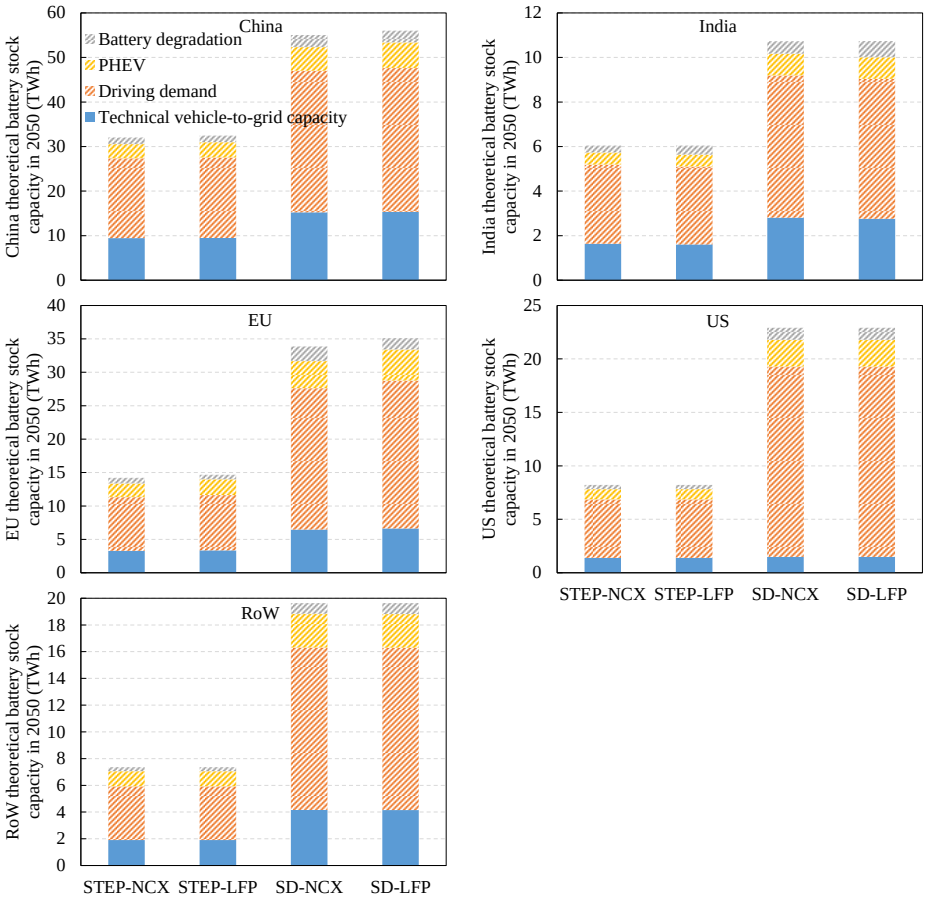

Supplementary Fig. 5.15: Available vehicle-to-grid capacity in 2050 by countries/regions. Hatched bars indicate the capacity limits due to key factors and blue bars the technical vehicle-to-grid capacity. It is found higher technical vehicle-to-grid capacity for LFP scenario compared to NCX scenario in China, EU, and US, while higher vehicle-to-grid capacity for the NCX scenario in India and RoW (Rest of World).

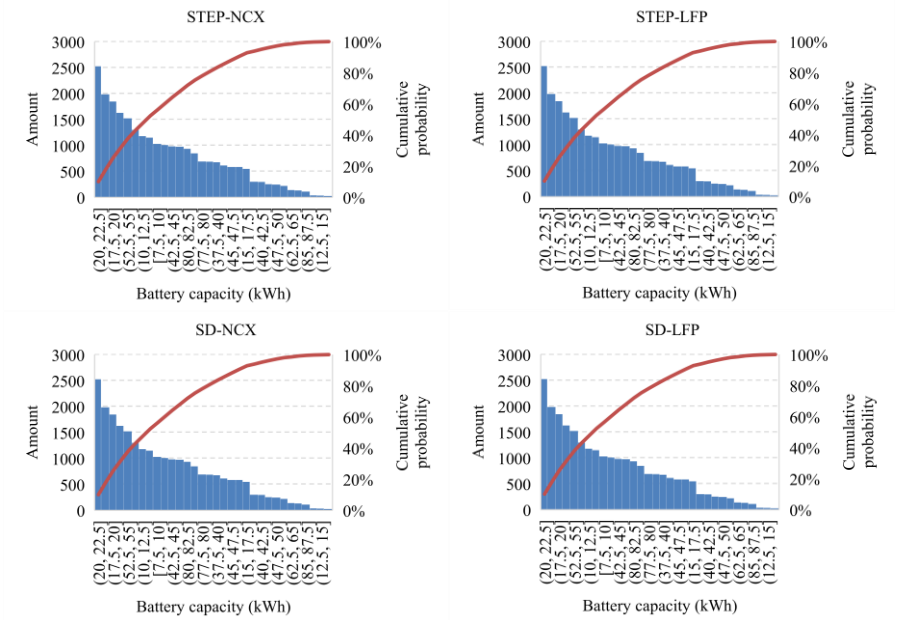

Supplementary Fig. 5.16: Battery capacity distribution for China battery stock by 2050.

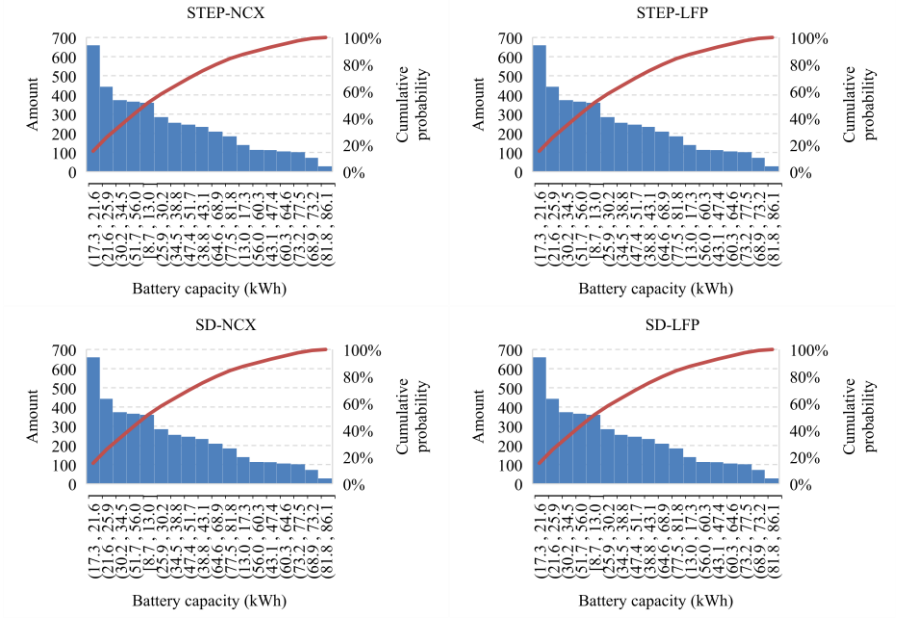

Supplementary Fig. 5.17: Battery capacity distribution for India battery stock by 2050.

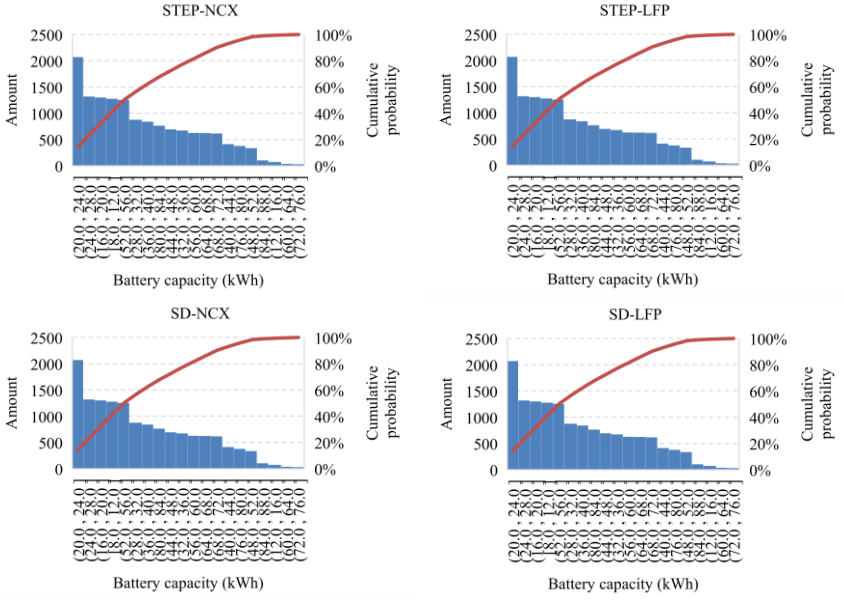

Supplementary Fig. 5.18: Battery capacity distribution for EU battery stock by 2050.

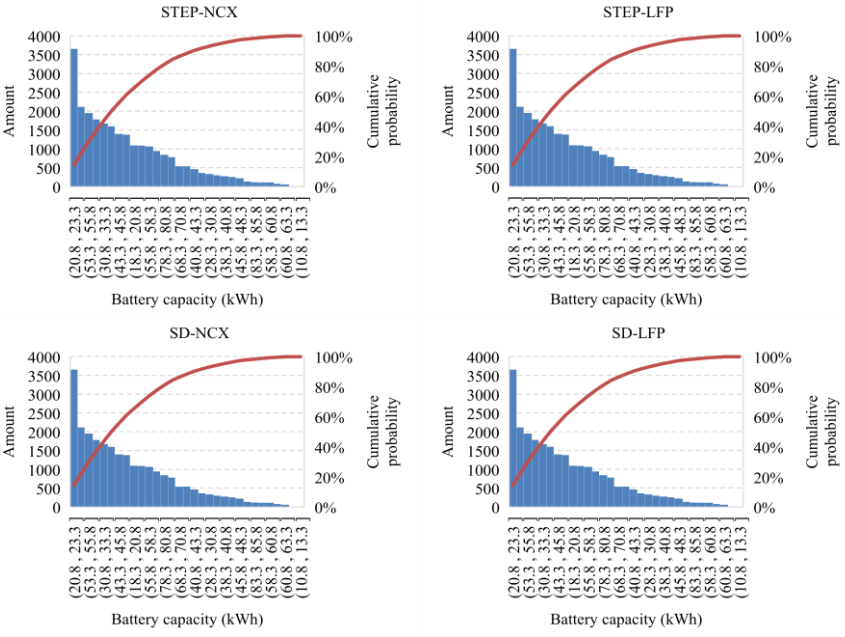

Supplementary Fig. 5.19: Battery capacity distribution for US battery stock by 2050.

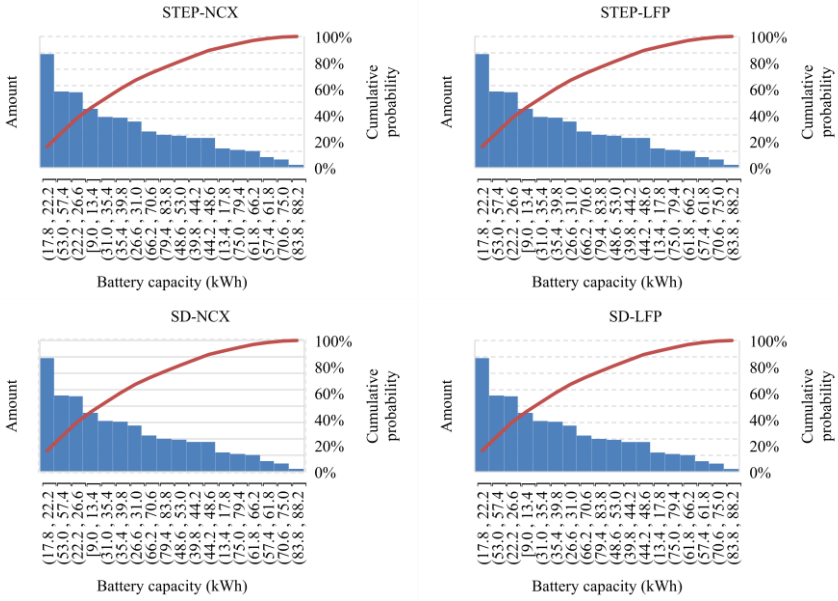

Supplementary Fig. 5.20: Battery capacity distribution for RoW battery stock by 2050.

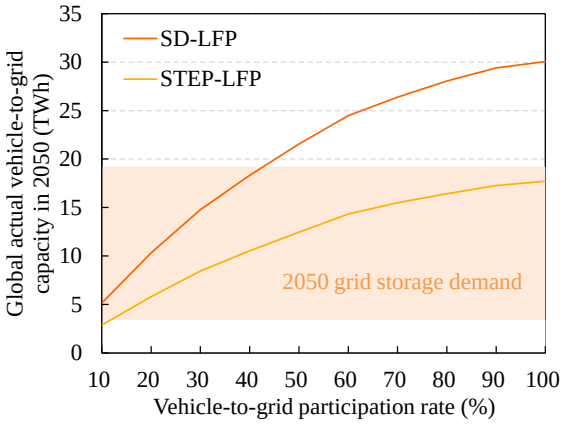

Supplementary Fig. 5.21: Global actual vehicle-to-grid capacity as a function of participation rates in STEP-LFP and SD-LFP scenarios, and comparison to grid storage capacity demand in 2050.

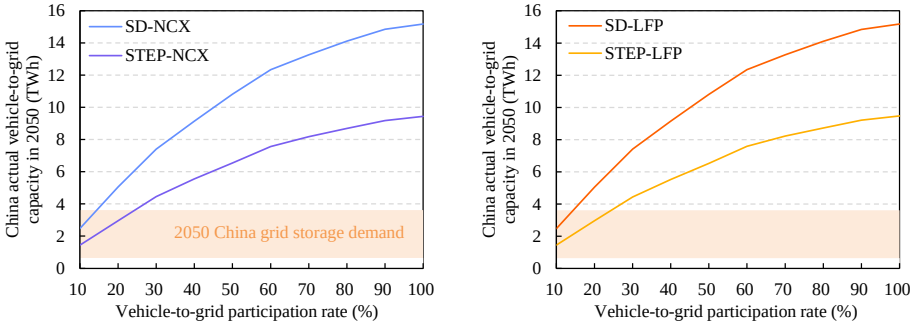

Supplementary Fig. 5.22: China actual vehicle-to-grid capacity as a function of participation rate and comparison to grid storage capacity demand in 2050.

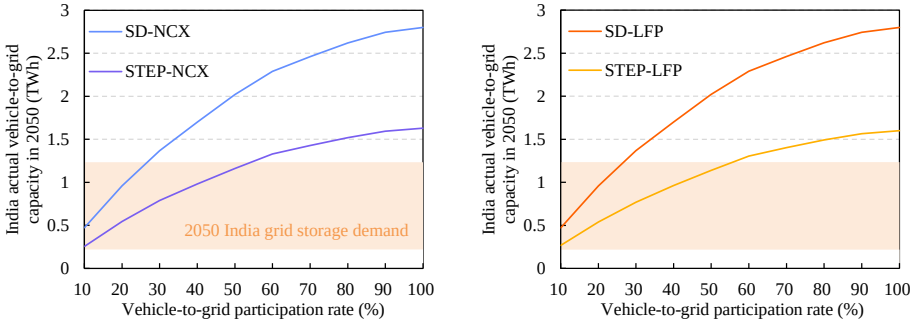

Supplementary Fig. 5.23: India actual vehicle-to-grid capacity as a function of participation rate and comparison to grid storage capacity demand in 2050.

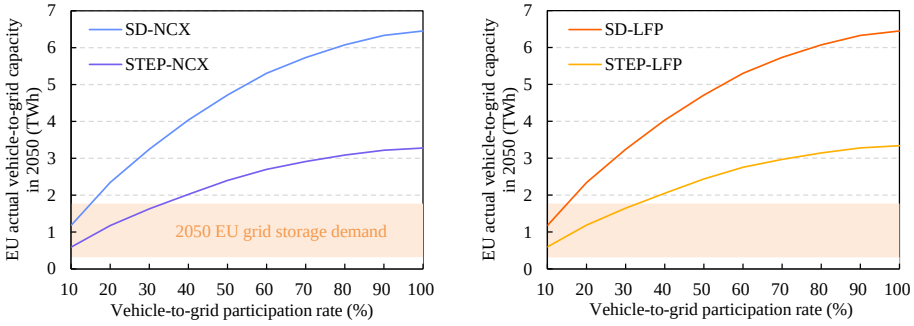

Supplementary Fig. 5.24: EU actual vehicle-to-grid capacity as a function of participation rate and comparison to grid storage capacity demand in 2050.

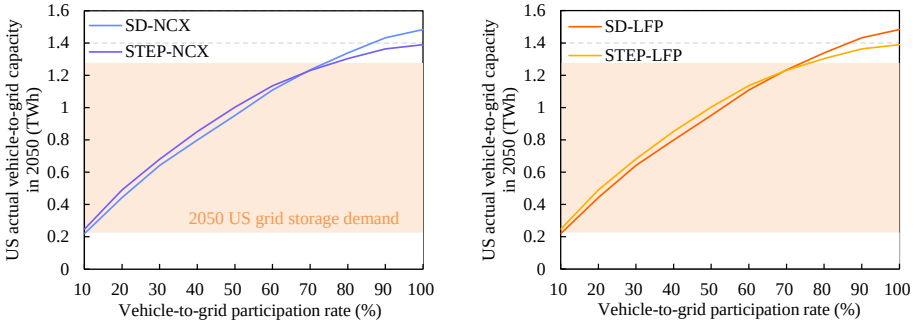

Supplementary Fig. 5.25: US actual vehicle-to-grid capacity as a function of participation rate and comparison to grid storage capacity demand in 2050.

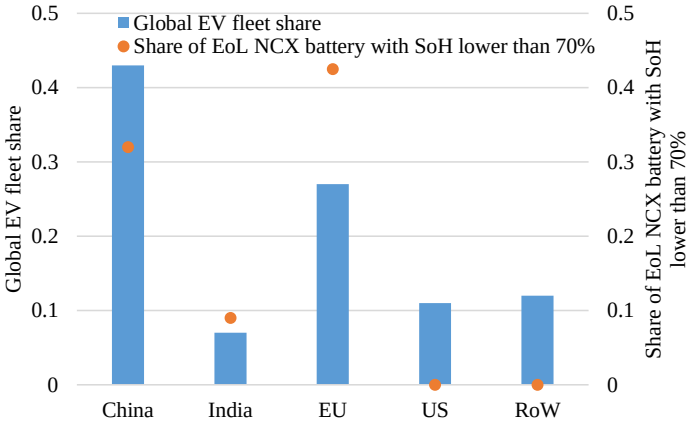

Supplementary Fig. 5.26: Global share of retired NCX batteries with SoH lower than 70% in total retired NCX batteries (*i.e.*, repurposing rate per year). Repurposing rate per year = number of collected batteries with relative SoH above 70% per year / number of collected batteries per year.

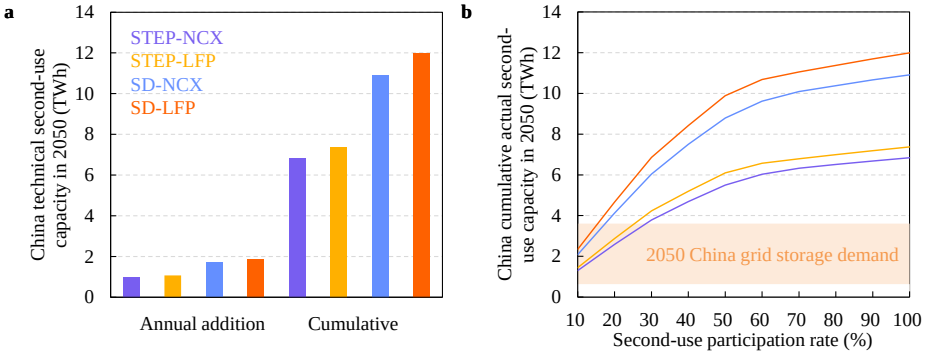

Supplementary Fig. 5.27: China available second-use capacity in 2050. a Annual addition and cumulative technical capacity in 2050. Capacity refers to the technically available capacity considering battery degradation, or maximum theoretical potential second-use capacity without considering the battery second-use participation rate. **b** Impacts of second-use participation rate on cumulative actual second-use capacity and a comparison to storage demand in 2050 (orange shading).

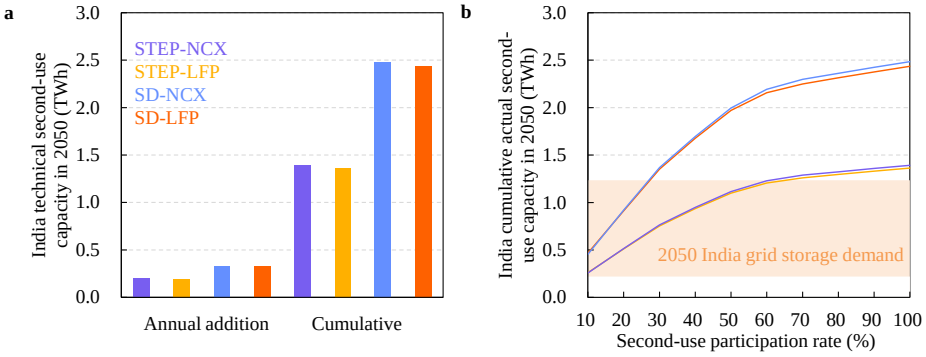

Supplementary Fig. 5.28: India available second-use capacity in 2050. a Annual addition and cumulative technical capacity in 2050. Capacity refers to the technically available capacity considering battery degradation, or maximum theoretical potential second-use capacity without considering the battery second-use participation rate. **b** Impacts of second-use participation rate on cumulative actual second-use capacity and a comparison to storage demand in 2050 (orange shading).

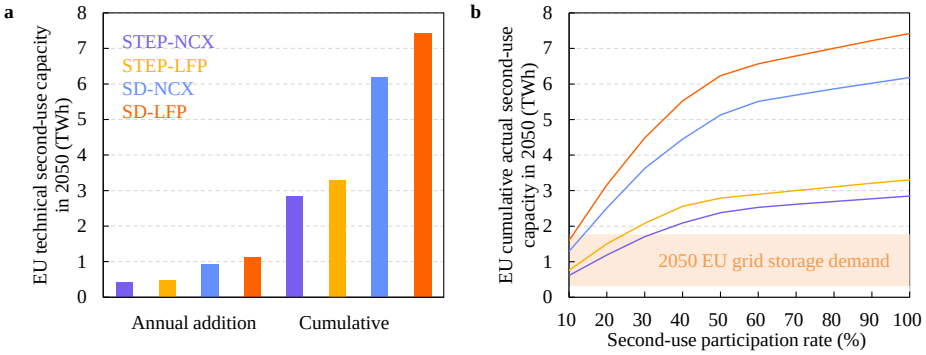

Supplementary Fig. 5.29: EU available second-use capacity in 2050. a Annual addition and cumulative technical capacity in 2050. Capacity refers to the technically available capacity considering battery degradation, or maximum theoretical potential second-use capacity without considering the battery second-use participation rate. **b** Impacts of second-use participation rate on cumulative actual second-use capacity and a comparison to storage demand in 2050 (orange shading).

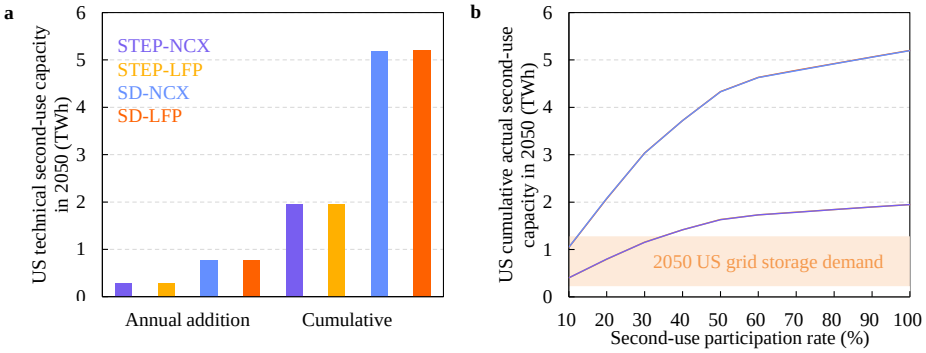

Supplementary Fig. 5.30: US available second-use capacity in 2050. a Annual addition and cumulative technical capacity in 2050. Capacity refers to the technically available capacity considering battery degradation, or maximum theoretical potential second-use capacity without considering the battery second-use participation rate. **b** Impacts of second-use participation rate on cumulative actual second-use capacity and a comparison to storage demand in 2050 (orange shading).

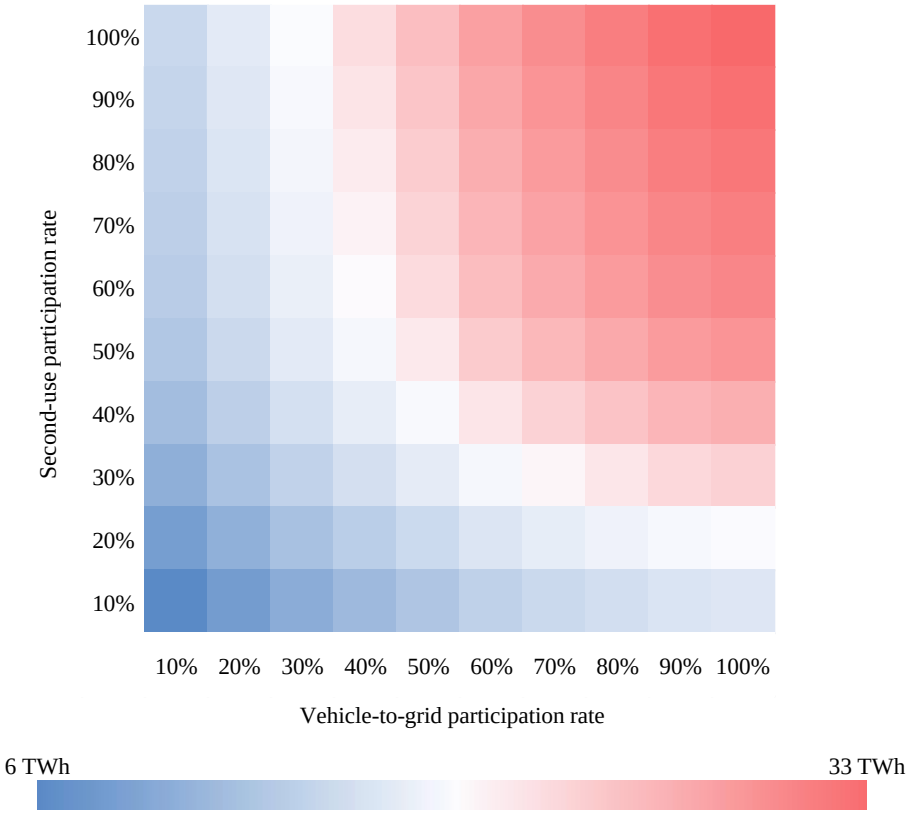

Supplementary Fig. 5.31: Total actual available capacity under various conditions in STEP-LFP scenario in 2050. Blue, white, and red colors depict minimum, average, and maximum values.

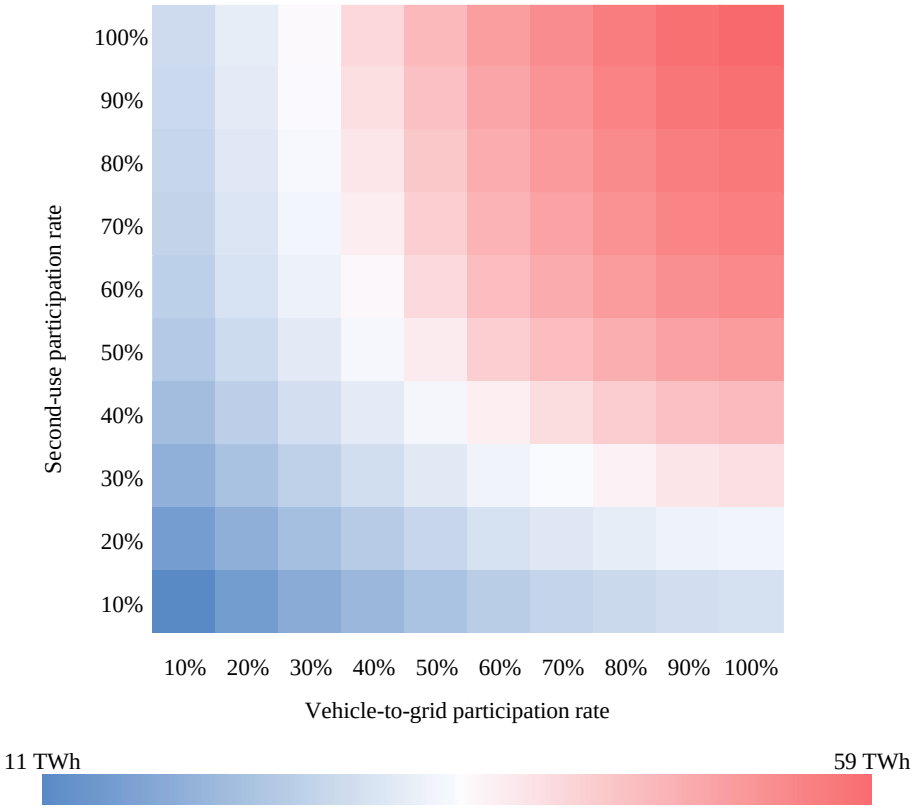

Supplementary Fig. 5.32: Total actual available capacity under various conditions in SD-NCX scenario in 2050. Blue, white, and red colors depict minimum, average, and maximum values.

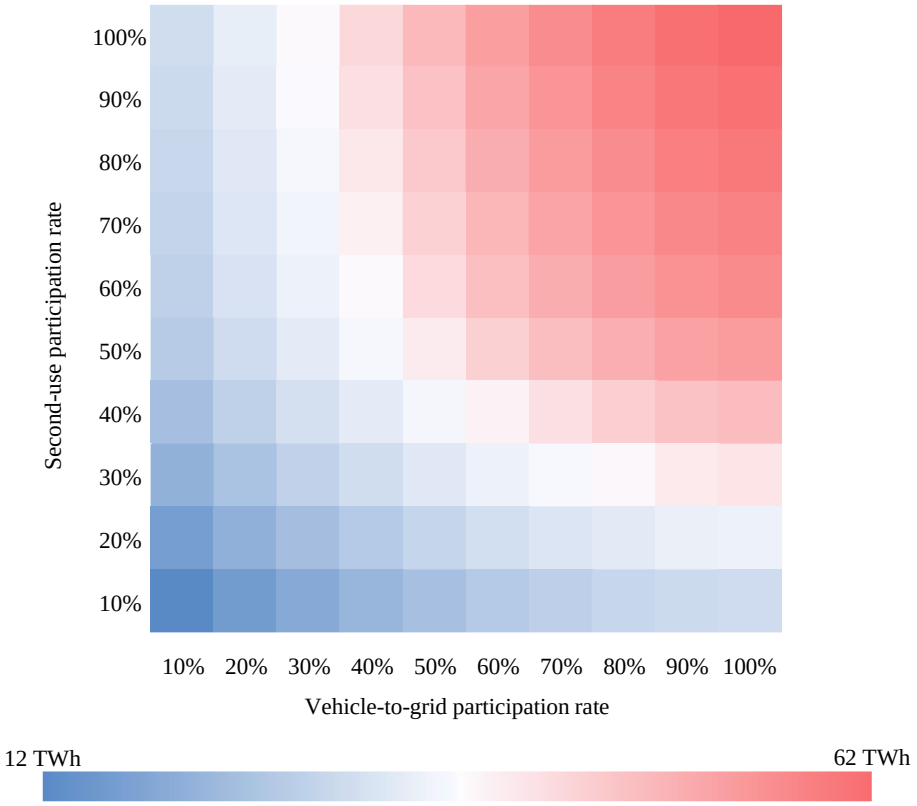

Supplementary Fig. 5.33: Total actual available capacity under various conditions in SD-LFP scenario in 2050. Blue, white, and red colors depict minimum, average, and maximum values.

Supplementary Table

Supplementary Table 5.1: Future grid storage capacity demand. IEA = International Energy Agency. IRENA = International Renewable Energy Agency. BNEF = Bloomberg New Energy Finance. SD scenario = sustainable development scenario. Remap = Renewable Energy Roadmap. PES = Planned Energy Scenario. The "Planned Energy Scenario (PES)" is the primary reference case for this study, providing a perspective on energy system developments based on governments' current energy plans and other planned targets and policies (as of 2019), including Nationally Determined Contributions under the Paris Agreement unless the country has newer climate and energy targets or plans. TES = Transforming Energy Scenario. The "Transforming Energy Scenario (TES)" describes an ambitious, yet realistic, energy transformation pathway based largely on renewable energy sources and steadily improved energy efficiency (though not limited exclusively to these technologies). This would set the energy system on the path needed to keep the rise in global temperatures to well below 2 degree Celsius (°C) and towards 1.5°C during this century. Unit: TWh. TWh = 10^9 kWh.

Reference	Capacity demand	Scenarios	2030	2040	2050	Annual growth rate /increasing factor in 2030~2050	Annual growth rate /increasing factor in 2040~2050
IEA[235]	Stationary storage batteries	SD	/	2.9884	/		
IRENA[236]	Behind the meter storage batteries	Remap	/	/	9		
IRENA[237]	Electricity storage energy capacity	Reference scenario	7.22	/	/		
IRENA[237]	Electricity storage energy capacity	Doubling scenario	13.58	/	/		
IRENA[56]	Stationary storage	PES	0.37	/	3.4	0.12/9.19	

Supplementary Table 5.1 (Continued).

Reference	Capacity demand	Scenarios	2030	2040	2050	Annual growth rate /increasing factor in 2030~2050	Annual growth rate /increasing factor in 2040~2050
IRENA[56]	Stationary storage	TES	0.745	/	9	0.13/12.08	
BNEF[238]	Energy storage installations	/	/	2.85	/		
Storage Lab[194]	Flexibility grid storage capacity	Optimistic approaches	/	2.8	8.8		0.12/3.14
Storage Lab[194]	Flexibility grid storage capacity	Conservative approaches	/	8.8	19.2		0.08/2.18

Supplementary Table 5.2: Selected EV models for modeling daily driving distance (DDD) distributions and driving cycles.

Vehicle type and class	EV models for modeling DDD distribution	Representative model for modeling drive cycles
Small BEV	Smart fortwo, Mitsubishi i-MiEV, BMW i3, Volkswagen e-Golf	Mitsubishi i-MiEV
Mid-size BEV	Nissan Leaf, Mercedes-Benz B250e, Honda Clarity EV, Hyundai Ioniq Electric, Tesla Model 3	Nissan Leaf 30 kWh
Large BEV	Tesla Model S, Kia Soul Electric, Hyundai Kona Electric	TESLA Model S60 2WD
PHEV	Toyota Prius, Ford C-MAX Energi Plug-In Hybrid, Hyundai Ioniq Plug-in Hybrid	Prius Prime

Supplementary Table 5.3: Optimized parameters for LFP and NCM degradation model.

Parameter	LFP	NCM
k_{Cal}	1.9234E-3 ($days^{0.5}$)	4.0149E-4 ($days^{0.5}$)
E_a	3.0233E4 (J/mol·K)	5.9178E4 (J/mol·K)
α	-0.05590	-1
k_{Cyc}	2.93583E-6	4.3131332E-6
A	1.4761E-11	0.3549361
B	7.4008E-3	1.2308964E-4
C	0.082035	0
D	0.0313111	1
E	0.33344256	0.6149392
F	331.652158	63.619859

5.5.3 Supplementary Notes

Supplementary Note 5.1

As shown in Supplementary Fig. 4, we compile the trip driving cycle based on a standard US combined driving cycle (*i.e.*, 55% UDDS city driving and 45% HWY highway driving). We first model the required trip distance and time for UDDS city driving and HWY highway driving, respectively. By comparing the required driving distance with the distance of the standard driving cycle, the required multiples (*i.e.*, the repeated times of standard UDDS or HWY driving cycle) and downsizing factor (the downscaling of standard UDDS or HWY driving cycle to satisfy a small driving distance) are modeled, respectively, thus scaling up or down of standard driving cycle to the required driving distance. Supplementary Fig. 5 shows the driving cycle example of

mid-size BEV, where the mean driving distance between 33%-50% EV range is 126.3 km. A 63.1 km of trip distance requires 2 multiples of standard UDDS city driving and 1 multiple of standard HWY highway driving, as well as 1 downsized standard UDDS driving distance with a downsizing factor of 1.11 and 1 downsized standard HWY driving with a downsizing factor of 1.38.

Supplementary Note 5.2

According to degradation models fit with aging data from state-of-the-art NCM and LFP batteries, LFP batteries show lower levels and less variance of degradation than NCX as LFP is less sensitive to temperature variation, state-of-charge, and depth of discharge in both calendar-life and cycle-life degradation rates (Supplementary Figs. 32 and 33). For a mid-size battery electric vehicle (BEV), an increase of daily driving distance (DDD) from 0%-25% EV range to 100%-200% of EV range could reduce the relative battery State-of-health (SoH) at 8 years (*i.e.*, battery lifetime warranty by most EV manufacturers) by 5.5-22% for NCM and 1-1.5% for LFP, depending on temperature conditions (see Supplementary Data for degradation for different EV size and type). Higher utilization of plug-in hybrid vehicle (PHEV) batteries leads to higher degradation for PHEV batteries than for BEV batteries. Battery degradation variations among countries/regions are driven by driving intensity and climate conditions; the lifetime of NCM batteries in Europe is expected to be substantially shorter than other regions due to increased degradation caused by cycling at low average temperatures, while the lifetime of LFP batteries is shortest in India due to increased calendar degradation rate at high average temperatures (see Supplementary Figs. 28~31 for DDD distributions, Supplementary Data for city temperature and battery degradation).